

**Extracting ergotropy from nonequilibrium steady states of an  $XXZ$  spin-chain quantum battery**B. Mojaveri <sup>\*</sup>, R. Jafarzadeh Bahrbeig,<sup>†</sup> and M. A. Fasihi <sup>‡</sup>*Department of Physics, Azarbaijan Shahid Madani University, P.O. Box 51745-406, Tabriz, Iran* (Received 18 September 2023; revised 15 January 2024; accepted 22 March 2024; published 15 April 2024)

Coupling of a quantum battery (QB) to two thermal reservoirs brings it to a nonequilibrium steady-state (NESS). In this situation, although, the QB can be charged through the NESS heat current, no work may be extracted from it through unitary cyclic processes. We exemplify this statement by studying the two- and three-qubit  $XXZ$  spin-chain QBs coupled weakly to two different thermal reservoirs in a symmetric configuration wherein each end of chain interacts with an individual reservoir. We show that the work can be extracted at positive temperature bias when two ends of a  $XXZ$  chain are collectively coupled to the hot reservoir.

DOI: [10.1103/PhysRevA.109.042619](https://doi.org/10.1103/PhysRevA.109.042619)**I. INTRODUCTION**

In recent years, with advancements in quantum thermodynamics, there has been a radical change of perspective in the framework of energy manipulation based on the electrochemical principles. The possibility to create an alternative and efficient energy storage device at small scale introduces the concept of the quantum battery (QB), which was proposed by Alicki and Fannes in 2013 [1] and subsequently became a significant field of research. As their name indicates, QBs are finite-dimensional quantum systems that are able to temporarily store energy in their quantum degrees of freedom for later use. Indeed, the key point here is that nonclassical features such as quantum coherence, entanglement, and many-body collective behaviors can be used to obtain more efficient and faster charging processes than the macroscopic counterpart. During the last years, studies on the QBs have been generalized in different directions. They included proposing the theoretical schemes [2–10], examining performance of such devices by analyzing some figures of merit such as the charging power (energy stored in a given time interval) [11,12], and ergotropy (the maximum amount of energy which can be extracted via cyclic unitary transformations) [13–15], advising an appropriate control strategy to achieve a quantum charging advantage [16–24], and discussing the environmental induced decoherence on charging and discharging processes of QBs [25–31]. At the same time, several experimental schemes have been also proposed to implement QBs based on the two-level systems such as trapped ions [8,32,33], cold atoms [34] and superconducting qubits [35].

One of the most important issues related to performance of QBs is their charging process, during which the system transits from a lower energy level into the higher ones. A QB is generally charged based on an interaction protocol

between QB itself with an external field which serves as a charger. So far, the main focus has lied on charging a QB by means coupling to other quantum systems [8] driving with an external field [36–39], unitary operations [11,40] as well as performing projective measurements [41]. Particularly interesting is charging by means the thermal environments [28], which would require much less control and greater stability in compare with the other ones. Considering that the battery undergoes an environmental-induced dissipation dynamics, charging by means the thermal environment portrays a positive role of decoherence in improving the potentialities of open QBs. However, this charging mechanism does not work when the quantum system is coupled to a Markovian thermal reservoir because it evolves the battery to the familiar Gibbs thermal states, which are the passive states (namely the states from which one cannot extract any energy by means of unitary transformations). In Ref. [2] Farina *et al.* have shown that indirect thermal charging, where the interaction between the battery and the thermal environment mediated by an ancilla system, may produce some active steady states. On the other hand, the steady state of a composite system in contact with two or more independent thermal baths does not obey the Gibbs distribution, so it is expected that, under the proper circumstances, active steady states could be produced out of thermal equilibrium. Generally, moving out of the thermal equilibrium induces heat current among the interacting subsystems which may changes the steady-state population distribution among the eigenstates of composite systems [42], and potentially produces a non-Gibbsian active state under the proper conditions [43,44].

In this paper, we show that presence of an inherent asymmetry induced by the asymmetrically couplings of a QB to two independent reservoirs results in a finite ergotropy of nonequilibrium steady state (NESS). Here, we propose an open QB modeled as a two-qubit  $XXZ$  spin chain coupled to two independent Markovian thermal reservoirs in two symmetrical coupling or asymmetrical coupling configurations. In the symmetrical coupling configuration, one qubit is coupled to only one reservoir, while in the asymmetrical coupling configuration, one of qubits is coupled to the both reservoirs

<sup>\*</sup>Corresponding author: [bmojaveri@azaruniv.ac.ir](mailto:bmojaveri@azaruniv.ac.ir);  
[bmojaveri@gmail.com](mailto:bmojaveri@gmail.com)

<sup>†</sup>[r.jafarzadeh86@gmail.com](mailto:r.jafarzadeh86@gmail.com)

<sup>‡</sup>[a.fasihi@gmail.com](mailto:a.fasihi@gmail.com)

and the other only to one reservoir. The battery is initiated in a state in which both qubits are in its ground state. The battery is charged through both the environmental induced decoherence in their energy eigenbasis as well as incoherent heat flow resulting from the weak coupling of the qubits to the reservoirs at different temperatures. However, in the equilibrium case (i.e., when temperature difference of reservoirs is zero), it is charged only by means environmental induced decoherence in their energy eigenbasis. We investigate how the mean temperature and temperature gradient of the reservoirs, as well as the chain anisotropy can affect the charging performance of QB in the steady-state limit. We analytically show that the steady state of the two-qubit spin-chain QB coupled symmetrically to the reservoirs is passive, while in the asymmetrical coupling configuration, it is possible to extract work through unitary cyclic processes. We confirm these results by numerical simulation of a three-qubit spin-chain counterpart. Our results present a robust way to generate and store ergotropy in a QB through relaxation of a nonequilibrium quantum system into its steady state by purely thermal means while assuming a weak but asymmetrical coupling between the system and its thermal reservoirs.

The rest of the paper is organized as follows: In Sec. II we introduce the model for a two-qubit spin-chain QB and derive in detail the Markovian master equation describing the nonequilibrium dynamics of system coupled to its thermal reservoirs. In Sec. III, we analyze the steady state stored energy in both the symmetric and asymmetric coupling settings with emphasis on the control role of the chain anisotropy and nonequilibrium effects. Then, we examine the ergotropy of the NESS of our battery in Sec. IV. In Sec. V, we analyze the charging performance of the battery for the case of three qubits. Finally, we draw some conclusions from the present study in Sec. VI. The proof of passivity of the two-qubit QB with symmetric qubit-reservoir coupling configuration can be found in the Appendix A. In addition, the emission and absorption rates between energy levels of the three-qubit QB, and the dynamical equations for its density-matrix elements are given in Appendixes B and C, respectively.

## II. THE MODEL AND ITS NONEQUILIBRIUM STEADY-STATE SOLUTIONS

We consider a QB composite of a two-qubit anisotropic  $XXZ$  spin chain in the presence of a uniform magnetic field  $B_0$ , which is described by the Hamiltonian

$$H_B = \frac{1}{2} [B_0 \sigma_z^{(1)} + B_0 \sigma_z^{(2)} + J \sigma_x^{(1)} \sigma_x^{(2)} + J \sigma_y^{(1)} \sigma_y^{(2)} + \Delta \sigma_z^{(1)} \sigma_z^{(2)}], \quad (1)$$

where  $\sigma_x^{(i)}$ ,  $\sigma_y^{(i)}$ , and  $\sigma_z^{(i)}$  are spin 1/2 operators for the  $i$ th spin, and  $B_0$  is a magnetic field in the  $z$  direction.  $J$  is the interqubit coupling and  $(-1 \leq \Delta \leq 1)$  denotes the chain anisotropy in the  $z$  direction. For  $J > 0$  and  $\Delta > 0$  the chain is called anti-ferromagnetic while for  $J < 0$  and  $\Delta < 0$  it is a ferromagnetic chain [45,46]. Remarkably, for the particular values  $\Delta = 0$  and  $\Delta = J$ , the Hamiltonian (1) corresponds to the  $XX$  [47] and  $XXX$  [48] spin chains, respectively. The eigenenergies

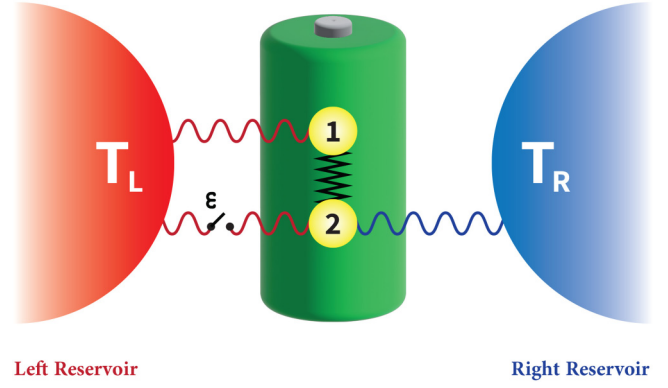


FIG. 1. The schematic diagram of the  $XXZ$  spin-chain QB with two coupled qubits 1 and 2 interacting with a nonequilibrium environment consists of left and right reservoirs. The key  $\epsilon$  is used to switch on or of f the coupling between the qubit 2 and left reservoir, which allow us to control chain-reservoir coupling asymmetry.

and corresponding eigenbasis of  $H_B$  in the two-qubit bare basis  $\{|1, 1\rangle, |1, 0\rangle, |0, 1\rangle, |0, 0\rangle\}$  are

$$|\Phi_1\rangle = |0, 0\rangle, \quad E_1 = \frac{1}{2}(\Delta - 2B_0), \quad (2a)$$

$$|\Phi_2\rangle = |1, 1\rangle, \quad E_2 = \frac{1}{2}(\Delta + 2B_0), \quad (2b)$$

$$|\Phi_3\rangle = \frac{1}{\sqrt{2}}[|0, 1\rangle - |1, 0\rangle], \quad E_3 = -\frac{\Delta}{2} - J, \quad (2c)$$

$$|\Phi_4\rangle = \frac{1}{\sqrt{2}}[|1, 0\rangle + |0, 1\rangle], \quad E_4 = -\frac{\Delta}{2} + J. \quad (2d)$$

In the bare basis  $\{|1, 1\rangle, |1, 0\rangle, |0, 1\rangle, |0, 0\rangle\}$ , the Hamiltonian  $H_B$  can be represented as

$$H_B = \begin{pmatrix} \frac{\Delta+2B_0}{2} & 0 & 0 & 0 \\ 0 & -\frac{\Delta}{2} & J & 0 \\ 0 & J & -\frac{\Delta}{2} & 0 \\ 0 & 0 & 0 & \frac{\Delta-2B_0}{2} \end{pmatrix}. \quad (3)$$

Figure 1 illustrates a schematic diagram of the nonequilibrium charging protocol of the QB. As can be seen, a coupling switch is used to provide the nonequilibrium charging of QB in two independent protocols. In the first charging protocol where the switch is off, the battery's qubits are coupled symmetrically to the left (right) reservoirs  $\mathcal{R}_L$  ( $\mathcal{R}_R$ ) with temperatures  $T_L$  ( $T_R$ ). The qubit 1 is coupled with the left reservoir and the qubit 2 interacts with the right reservoir. In the second protocol, the switch is flipped on, and an extra coupling between the qubit 2 and the left reservoir will be established. At this time, the qubits are coupled to the reservoirs in an asymmetric configuration wherein qubit 2 interacts with both reservoirs, whereas the qubit 1 is coupled to just the left reservoir. The left and right heat reservoirs are modeled as a collection of independent harmonic oscillators with the mode frequencies  $\omega_j^{(L)}$  and  $\omega_j^{(R)}$ , respectively, and described by the Hamiltonian ( $\hbar = 1$  and  $k_B = 1$  in the following)

$$H_{\text{res}} = \sum_j [\omega_j^{(L)} a_j^\dagger a_j + \omega_j^{(R)} b_j^\dagger b_j], \quad (4)$$

where  $a_j^\dagger$  ( $a_j$ ) and  $b_j^\dagger$  ( $b_j$ ) are the creation (annihilation) operators associated with the  $j$ th bosonic mode of the left and right reservoir, respectively. For simplicity, we just consider the dissipative interaction between the system and environment inducing the energy exchange between the qubits and corresponding local reservoirs and exclude pure dephasing type environmental noises. The dissipative interaction between the battery and the thermal reservoirs is described by the Hamiltonian

$$H_{\text{B-res}} = \sum_j \lambda_j^{(L)} (\sigma_x^{(1)} + \varepsilon \sigma_x^{(2)}) (a_j^\dagger + a_j) + \sum_j \lambda_j^{(R)} \sigma_x^{(2)} (b_j^\dagger + b_j), \quad (5)$$

where  $\lambda_j^{(L)}$  ( $\lambda_j^{(R)}$ ) is the dissipative interaction strength between the QB and the left (right) reservoirs. In addition,  $\varepsilon$

is a switching parameter which gets 0 or 1. Precisely,  $\varepsilon = 0$  switches off the interaction between the qubit 2 and the left reservoir. In this situation we have a symmetric configuration, the qubit 1 interacts only with the left reservoir and the qubit 2 interacts only with the right one. However,  $\varepsilon = 1$  switches on the coupling between the qubit 2 and the left reservoir and induces an inherent asymmetry in the qubit-reservoir coupling. In such an asymmetric coupling setting the qubit 1 interacts only with the left reservoir, while the qubit 2 interacts simultaneously with both the left and right reservoirs.

We now assume that the battery-reservoir interaction strength is in the weak-coupling regime, so under the Born-Markov approximation, the dynamics of QB can be described by the following Lindblad-form master equation [49]

$$\dot{\rho}(t) = -i[H_B, \rho(t)] + \mathfrak{D}_L(\rho) + \mathfrak{D}_R(\rho), \quad (6)$$

where  $\mathfrak{D}_\nu(\rho)$ , ( $\nu = L, R$ ) are dissipators associated with the reservoir  $\mathcal{R}_\nu$  in contact with the qubits, and take the form as

$$\begin{aligned} \mathfrak{D}_\nu(\rho) = & \sum_{\omega>0} \mathcal{J}_\nu(\omega)(1+n_\nu(\omega)) \left[ A_\nu(\omega) \rho(t) A_\nu^\dagger(\omega) - \frac{1}{2} \{A_\nu^\dagger(\omega) A_\nu(\omega), \rho(t)\} \right] \\ & + \sum_{\omega>0} \mathcal{J}_\nu(\omega) n_\nu(\omega) \left[ A_\nu^\dagger(\omega) \rho(t) A_\nu(\omega) - \frac{1}{2} \{A_\nu(\omega) A_\nu^\dagger(\omega), \rho(t)\} \right]. \end{aligned} \quad (7)$$

Here  $\mathcal{J}_\nu(\omega) = \pi \sum_j |\lambda_j^\nu|^2 \delta(\omega - \omega_j^{(\nu)})$  is the spectral density of the reservoir  $\mathcal{R}_\nu$  and  $n_\nu(\omega) = [e^{\omega/T_\nu} - 1]^{-1}$  denotes the average particle number on frequency  $\omega$  in that reservoir. In addition,  $A_\nu(\omega)$  and  $A_\nu^\dagger(\omega)$  are the Lindblad operators which are chosen according to the form of the interaction Hamiltonian  $H_{\text{B-res}}$  in Eq. (5) to satisfy  $A_\nu(\omega) = A_\nu^\dagger(-\omega)$  and  $[H_B, A_\nu(\omega)] = -\omega A_\nu(\omega)$ . They are given by

$$A_L(\omega) = \sum_{\omega_{ij}=\omega>0} |\Phi_j\rangle \langle \Phi_j| (\sigma_x^{(1)} + \varepsilon \sigma_x^{(2)}) |\Phi_i\rangle \langle \Phi_i|, \quad (8a)$$

$$A_R(\omega) = \sum_{\omega_{ij}=\omega>0} |\Phi_j\rangle \langle \Phi_j| \sigma_x^{(2)} |\Phi_i\rangle \langle \Phi_i|, \quad (8b)$$

for all positive eigenfrequencies  $\omega = \omega_{ij} = E_i - E_j > 0$ , corresponding to the transitions  $|\Phi_i\rangle \rightarrow |\Phi_j\rangle$ . Substituting Eq. (7) into (6), and then using the Eqs. (8a) and (8b) we get

$$\dot{\rho}(t) = -i[H_B, \rho(t)] + \mathcal{L}_L^{(1)}(\rho) + \mathcal{L}_R^{(2)}(\rho) + \varepsilon(\mathcal{L}_L^{(2)}(\rho) + \mathcal{L}_L^{(1,2)}(\rho)), \quad (9)$$

where the dissipator  $\mathcal{L}_\nu^{(k)}(\rho)$  represents dissipation due to the qubit  $k$  coupled individually to the reservoir  $\mathcal{R}_\nu$ , while the dissipator  $\mathcal{L}_L^{(1,2)}(\rho)$  reflects the collective dissipation due to the qubits 1 and 2 commonly coupled to the left reservoir. The dissipators  $\mathcal{L}_\nu^{(k)}(\rho)$  and  $\mathcal{L}_L^{(1,2)}(\rho)$  have the following form

$$\begin{aligned} \mathcal{L}_\nu^{(k)}(\rho) = & \sum_{\omega>0} \mathcal{J}_\nu^{(k)}(\omega)(1+n_\nu(\omega)) \left[ V^{(k)}(\omega) \rho(t) V^{(k)\dagger}(\omega) - \frac{1}{2} \{V^{(k)\dagger}(\omega) V^{(k)}(\omega), \rho(t)\} \right] \\ & + \sum_{\omega>0} \mathcal{J}_\nu^{(k)}(\omega) n_\nu(\omega) \left[ V^{(k)\dagger}(\omega) \rho(t) V^{(k)}(\omega) - \frac{1}{2} \{V^{(k)}(\omega) V^{(k)\dagger}(\omega), \rho(t)\} \right], \end{aligned} \quad (10a)$$

$$\begin{aligned} \mathcal{L}_L^{(1,2)}(\rho) = & \sum_{\omega>0} \mathcal{J}_L^{(1,2)}(\omega)(1+n_L(\omega)) \left[ V^{(1)}(\omega) \rho(t) V^{(2)\dagger}(\omega) - \frac{1}{2} \{V^{(2)\dagger}(\omega) V^{(1)}(\omega), \rho(t)\} \right] \\ & + \sum_{\omega>0} \mathcal{J}_L^{(1,2)}(\omega) n_L(\omega) \left[ V^{(1)\dagger}(\omega) \rho(t) V^{(2)}(\omega) - \frac{1}{2} \{V^{(2)}(\omega) V^{(1)\dagger}(\omega), \rho(t)\} \right] \end{aligned}$$

$$\begin{aligned}
 & + \sum_{\omega>0} \mathcal{J}_L^{(1,2)}(\omega)(1+n_L(\omega)) \left[ V^{(2)}(\omega) \rho(t) V^{(1)\dagger}(\omega) - \frac{1}{2} \{V^{(1)\dagger}(\omega) V^{(2)}(\omega), \rho(t)\} \right] \\
 & + \sum_{\omega>0} \mathcal{J}_L^{(1,2)}(\omega) n_L(\omega) \left[ V^{(2)\dagger}(\omega) \rho(t) V^{(1)}(\omega) - \frac{1}{2} \{V^{(1)}(\omega) V^{(2)\dagger}(\omega), \rho(t)\} \right],
 \end{aligned} \tag{10b}$$

$$V^{(k)}(\omega) = \sum_{\omega>0} |\Phi_j\rangle \langle \Phi_j | \sigma_x^{(k)} | \Phi_i\rangle \langle \Phi_i|, \tag{10c}$$

where  $V^{\dagger(k)}(\omega_{ij})$  and  $V^{(k)}(\omega_{ij})$  are transition operators which describe respectively processes in which the QB receives energy from the reservoir  $\mathcal{R}_v$  through an excitation of the qubit  $k$  or dissipates energy to it through a deexcitation of that qubit. They are eigenoperators of  $H_B$ , that satisfy  $V^{(k)}(\omega_{ij}) = V^{\dagger(k)}(-\omega_{ij})$  and  $[H_B, V^{(k)}(\omega_{ij})] = -\omega_{ij} V^{(k)}(\omega_{ij})$ . In addition,  $\mathcal{J}_L^{(1,2)}(\omega) = [\mathcal{J}_L^{(1)}(\omega) \mathcal{J}_L^{(2)}(\omega)]^{1/2} = \mathcal{J}_L(\omega)$  represents collective damping rate of the qubits 1 and 2 induced by the left reservoir.

In the following we are interested in the Ohmic dissipation,  $\mathcal{J}_v(\omega) = \kappa\omega$ , where  $\kappa$  is a dimensionless constant which quantifies dissipation strength. It should be noted that in order to guarantee the validity of the Markovian approximation,  $\kappa$  needs to satisfy the condition  $\kappa \ll \{B_0, J, \Delta\}$ . By substituting Eqs. (10a), (10b), and (3) into Eq. (6), the master equation reads

$$\dot{\rho}(t) = -i[H_B, \rho(t)] + \sum_{v=L,R} [\gamma_{31}^{(v,e)} L_{\tau_{13}} + \gamma_{31}^{(v,a)} L_{\tau_{31}} + \gamma_{14}^{(v,e)} L_{\tau_{14}} + \gamma_{14}^{(v,a)} L_{\tau_{41}} + \gamma_{23}^{(v,e)} L_{\tau_{32}} + \gamma_{23}^{(v,a)} L_{\tau_{23}} + \gamma_{24}^{(v,e)} L_{\tau_{42}} + \gamma_{24}^{(v,a)} L_{\tau_{24}}], \tag{11}$$

where  $\tau_{ij} = |\Phi_i\rangle \langle \Phi_j|$ ,  $L_X = X\rho X^\dagger - \frac{1}{2}\{\rho, X^\dagger X\}$ , and

$$\gamma_{ij}^{(L,e)} = \frac{\kappa\omega_{ij}(\varepsilon + (-1)^j)^2}{2} [1 + n_L(\omega_{ij})], \quad \gamma_{ij}^{(R,e)} = \frac{\kappa\omega_{ij}}{2} [1 + n_R(\omega_{ij})], \tag{12a}$$

$$\gamma_{ij}^{(L,a)} = \frac{\kappa\omega_{ij}(\varepsilon + (-1)^j)^2}{2} n_L(\omega_{ij}), \quad \gamma_{ij}^{(R,a)} = \frac{\kappa\omega_{ij}}{2} n_R(\omega_{ij}), \tag{12b}$$

where  $\gamma_{ij}^{(v,e)}$  ( $\gamma_{ij}^{(v,a)}$ ) is emission (absorption) rate from  $|\Phi_i\rangle$  to  $|\Phi_j\rangle$  ( $|\Phi_j\rangle$  to  $|\Phi_i\rangle$ ), thanks to the interaction of the battery with the reservoir  $v$ . From the above equations, we note that, the emission and absorption rates  $\gamma_{31}^{(L,e)}$ ,  $\gamma_{31}^{(L,a)}$ ,  $\gamma_{23}^{(L,e)}$ , and  $\gamma_{23}^{(L,a)}$  are zero in the presence of the asymmetry ( $\varepsilon = 1$ ). This means that the energy transition  $|\Phi_1\rangle \leftrightarrow |\Phi_3\rangle$  and  $|\Phi_2\rangle \leftrightarrow |\Phi_3\rangle$  induced by the hot (left) reservoir are impossible. All allowed energy transitions induced by the right and left reservoirs are depicted in Fig. 2, at which a four-level qudit will be populated due to the interaction with both the left and right reservoirs.

The steady-state solution  $d\rho/dt = 0$  for the QB can be obtained by rewriting the master equation in the Eq. (9) in the energy basis representation. The advantage of this representation is that the master equations for diagonal elements decouple from nondiagonal ones. For our system, all

coherence components (nondiagonal elements) of the density matrix vanish in the steady-state limit ( $t \rightarrow \infty$ ). As a consequence, the steady-state density matrix  $\rho_{\text{NESS}}$  in the energy basis representation is a diagonal matrix with the following diagonal elements

$$\rho_{11} = \frac{E_{31}\eta_1 + E_{41}\eta_2}{\eta_1(A_{31} + A_{41})} \rho_{33}, \tag{13a}$$

$$\rho_{22} = \frac{A_{23}\eta_1 + A_{24}\eta_2}{\eta_1(E_{23} + E_{24})} \rho_{33}, \tag{13b}$$

$$\rho_{33} = \left[ \frac{E_{31}\eta_1 + E_{41}\eta_2}{\eta_1(A_{31} + A_{41})} + \frac{A_{23}\eta_1 + A_{24}\eta_2}{\eta_1(E_{23} + E_{24})} + \frac{\eta_2}{\eta_1} + 1 \right]^{-1}, \tag{13c}$$

$$\rho_{44} = \frac{\eta_2}{\eta_1} \rho_{33}, \tag{13d}$$

where

$$\begin{aligned}
 \eta_1 &= \frac{A_{31}E_{41}}{(A_{23} + E_{31})(A_{31} + A_{41})} + \frac{E_{23}A_{24}}{(A_{23} + E_{31})(E_{23} + E_{24})}, \\
 \eta_2 &= 1 - \frac{A_{31}E_{31}}{(A_{23} + E_{31})(A_{31} + A_{41})} \\
 &\quad - \frac{E_{23}A_{23}}{(A_{23} + E_{31})(E_{23} + E_{24})}, \\
 A_{ij} &= \gamma_{ij}^{(L,a)} + \gamma_{ij}^{(R,a)}, \quad E_{ij} = \gamma_{ij}^{(L,e)} + \gamma_{ij}^{(R,e)}.
 \end{aligned} \tag{14}$$

Now we have all the expressions in hand required to analyze the charging performance of the proposed spin chain QB in the NESS. In the following, we want to explore the nonequilibrium effects on the steady-state activation and steady-state

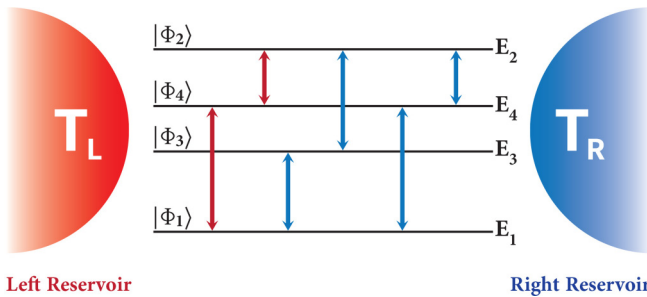


FIG. 2. Level structure of the QB asymmetrically coupled to the left and right reservoirs (the case  $\varepsilon = 1$ ). Red (blue) arrows indicate the allowed transitions in the interaction with the hot (cold) reservoir.

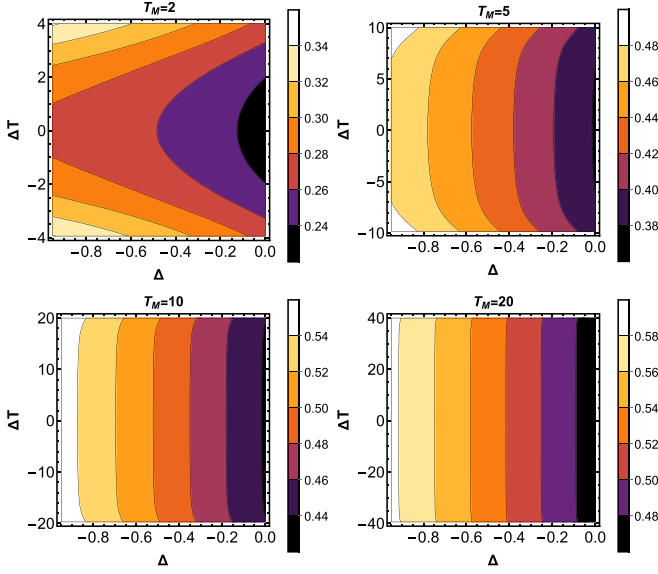


FIG. 3. The stored energy  $\Delta E_B(\infty)$  in the NESS of a ferromagnetic  $XXZ$  QB versus  $\Delta$  and  $\Delta T$  for different values of  $T_M$  in the symmetric coupling setting. The uniform magnetic field is set as  $B_0 = 2$ . All parameters of QB are in units of interspin coupling  $|J| = 1$ .

charging performances of a two-qubit  $XXZ$  spin-chain QB. Specially, we investigate how to improve the NESS charging performance of the QB by the introducing an inherent asymmetry induced by turning the coupling of qubit 2 to the left thermal reservoir, and find the proper circumstances to optimize the stored energy as well as ergotropy of QB. Furthermore, we show how such an asymmetry leads to the generation of active states that would be impossible to generate without such coupling.

To follow with the computation, we have to specify the initial state of QB. We assume here the battery is prepared initially in its ground state  $|\Phi_1\rangle = |0, 0\rangle$ , where both spins are in their ground states. Therefore, in order to charge the battery, the system parameters have to be adjusted in the regime of strong magnetic field  $B > |J + \Delta|$ .

### III. ENERGY STORED IN THE NONEQUILIBRIUM STEADY STATE OF THE $XXZ$ SPIN-CHAIN QUANTUM BATTERY

First, we investigate the nonequilibrium effects on the steady-state stored energy of ferromagnetic ( $J < 0$  and  $\Delta < 0$ ) and antiferromagnetic ( $J > 0$  and  $\Delta > 0$ ) spin-chain QBs for the symmetric coupling setting ( $\varepsilon = 0$ ). The energy stored in the QB, after a given time  $t$ , is evaluated from the quantum mechanics postulates [1] as

$$\Delta E_B(t) = \text{Tr}(\rho(t)H_B) - E_{gs}, \quad (15)$$

where  $\rho(t)$  is the density matrix of the battery at time  $t$  and  $E_{gs} = E_1 = \frac{1}{2}(\Delta - 2B_0)$  is the ground-state energy of the QB. In Fig. 3 (4) we plot the NESS stored energy  $\Delta E_B(\infty) = [E_B(\infty) - E_{gs}]/\Delta E_B^{\max}$  of a ferromagnetic (antiferromagnetic) spin-chain QB as a function of the temperature gradient of reservoirs  $\Delta T = T_L - T_R$  and the chain anisotropy

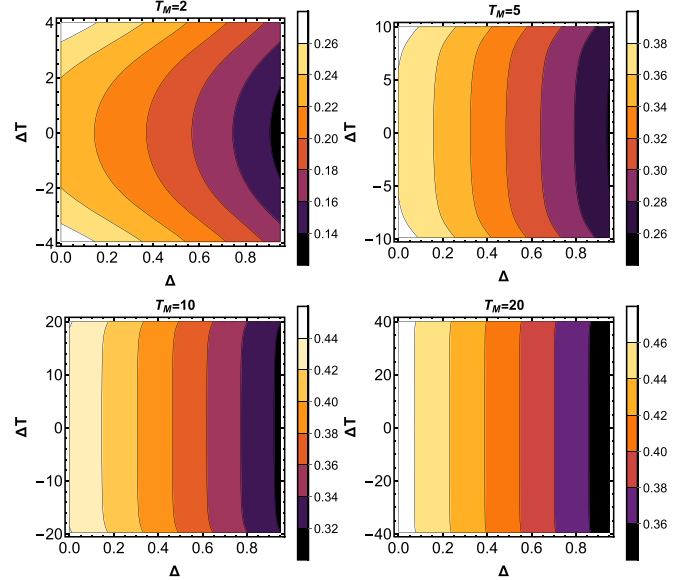


FIG. 4. The stored energy  $\Delta E_B(\infty)$  in the NESS of an antiferromagnetic  $XXZ$  QB versus  $\Delta$  and  $\Delta T$  for different values of  $T_M$  in the symmetric coupling setting. The uniform magnetic field is set as  $B_0 = 2$ . All parameters of QB are in units of interspin coupling  $|J| = 1$ .

$\Delta$  by considering different values of the mean temperature of reservoirs  $T_M = (T_L + T_R)/2$ . According to these figures, energy stored in the ferromagnetic and antiferromagnetic QBs can be controlled by the mean temperature of the reservoirs  $T_M$  as well as chain anisotropy  $\Delta$ ;  $\Delta E_B(\infty)$  increases with mean temperature of reservoirs. For a given  $T_M$ , the best energy storage in the steady state of the ferromagnetic and antiferromagnetic QBs are achieved, respectively, at  $\Delta \rightarrow -1$  and  $\Delta = 0$ . Interestingly, comparing Figs. 3 and 4 reveals that energy stored in the steady state of a ferromagnetic QB is more than that of the antiferromagnetic one.

Figures 3 and 4 also display a constructive role that the nonequilibrium effects play in enhancing the energy stored in the steady state of both ferromagnetic and antiferromagnetic QBs, albeit at the low mean temperatures (e.g.,  $T_M = 2$  in the figures). We clearly see that  $\Delta E_B(\infty)$  is symmetric in terms of the temperature gradient. This is expected because in the nonequilibrium regime, our QB is charged by means the heat current. And, based on the energy conservation at the steady state, the absorbed steady-state heat from the left (hot) reservoir is equal with the released steady-state heat to the right (cold) reservoir, which is the result of switching off the coupling between qubit 2 and the left reservoir.

In Figs. 5 and 6 we investigate NESS stored energy of the ferromagnetic and antiferromagnetic spin-chain QBs, respectively, for the asymmetric setting ( $\varepsilon = 1$ ). We here plot the steady-state stored energy  $\Delta E_B(\infty)$  as a function of  $\Delta T$  and  $\Delta$  for different values of the mean temperature  $T_M$ , comparing it with the symmetric couplings setting ( $\varepsilon = 0$ ). Obviously,  $\Delta E_B(\infty)$  is not symmetric in terms of the temperature gradient due to the fact that more heat current flows from the left reservoir to the right reservoir in the asymmetric-coupling setting [42]. It is evident that, similar to the symmetric coupling

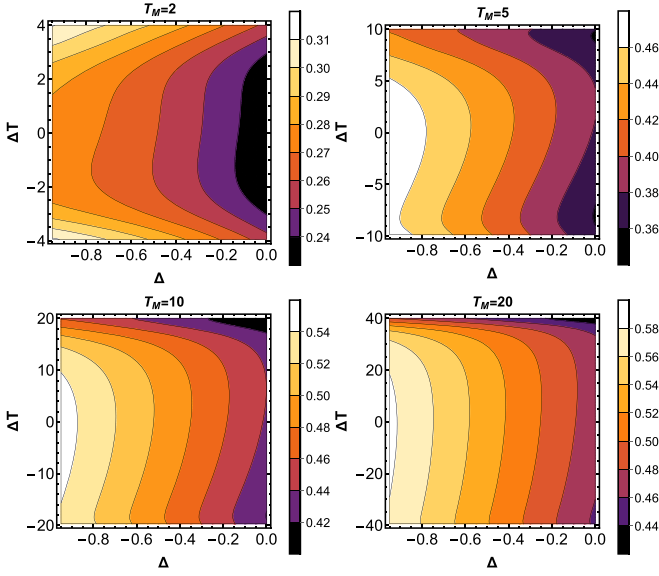


FIG. 5. The stored energy  $\Delta E_B(\infty)$  in the NESS of a ferromagnetic XXZ QB versus  $\Delta$  and  $\Delta T$  for different values of  $T_M$  in the asymmetric coupling setting. The uniform magnetic field is set as  $B_0 = 2$ . All parameters of QB are in units of interspin coupling  $|J| = 1$ .

setting, a constructive role of nonequilibrium effects of heat current in enhancing energy stored in the steady state of QBs is observed at low mean temperatures. By increasing mean temperature of reservoirs, however, the role of nonequilibrium effects of heat current changes from constructive to destructive, albeit at positive temperature bias. The destructive role of the heat current on the NESS stored energy, regardless of the ferromagnetic or antiferromagnetic properties of QB, is

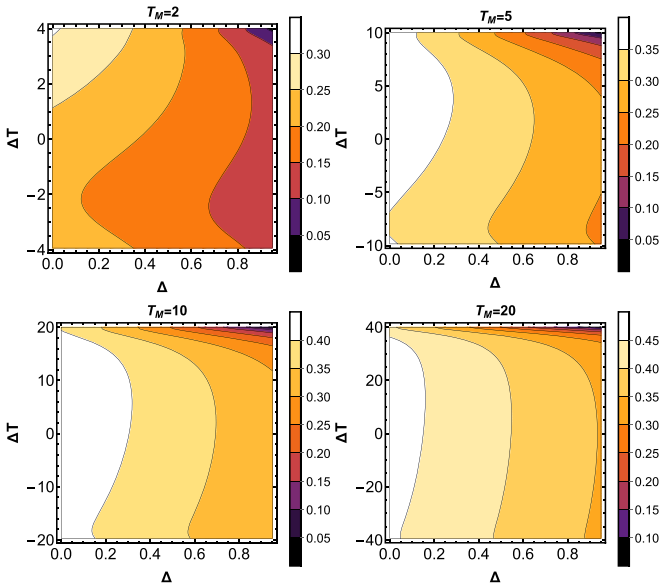


FIG. 6. The stored energy  $\Delta E_B(\infty)$  in the NESS of an antiferromagnetic XXZ QB versus  $\Delta$  and  $\Delta T$  for different values of  $T_M$  in the asymmetric coupling setting. The uniform magnetic field is set as  $B_0 = 2$ . All parameters of QB are in units of interspin coupling  $|J| = 1$ .

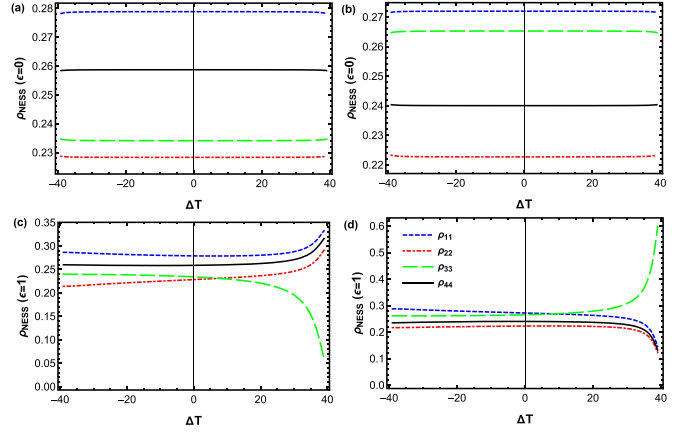


FIG. 7. NESS population distribution of the ferromagnetic [panels (a) and (c)] and antiferromagnetic [panels (b) and (d)] spin-based QB versus  $\Delta T$  by setting  $B_0 = 2$ ,  $T_M = 20$ , and  $\Delta = \pm 0.5$ . Panels (a) and (b) correspond to the symmetric spin-reservoir coupling setting, while panels (c) and (d) correspond to the asymmetric spin-reservoir coupling setting. All parameters of QB are in units of interspin coupling  $|J| = 1$ .

distributed unevenly across the chain anisotropy  $\Delta$ . Especially, in the antiferromagnetic QB, the destructive effects of the heat current are limited roughly at near  $\Delta T = 2T_M$ .

To gain a physical perspective on the features of  $\Delta E_B(\infty)$  in Figs. 3–6, we plot in Fig. 7 the NESS population in the eigenstate representation versus the temperature gradient  $\Delta T$  for  $T_M = 20$ ,  $B_0 = 2$ , and  $\Delta = \pm 0.5$ . We can see that in the symmetric coupling setting [see Figs. 7(a) and 7(b)] the steady-state population distribution of both ferromagnetic and antiferromagnetic QBs does not change with the temperature gradient and, therefore, the steady-state stored energy remain unchanged according to Eq. (15). In the asymmetric coupling setting, however, the steady-state population distribution is changed by the temperature gradient [see Figs. 7(c) and 7(d)], albeit at positive temperature bias. Figure 7(c) shows that, in the ferromagnetic QB the steady-state population components  $\rho_{11}$ ,  $\rho_{22}$ ,  $\rho_{44}$  ( $\rho_{33}$ ) increases (decreases) with  $\Delta T > 0$ . Taking into account that the eigenenergies  $E_2$  and  $E_3$  ( $E_1$  and  $E_4$ ) are positive (negative) for chosen the values of  $B_0 = 2$  and  $\Delta = -0.5$ , the increase in positive temperature gradient results in an increase in negative contribution of  $\rho_{11}E_1 + \rho_{33}E_3 + \rho_{44}E_4$  as well as the positive contribution of  $\rho_{22}E_2$ . In this situation, the negative contribution of  $\rho_{11}E_1 + \rho_{33}E_3 + \rho_{44}E_4$  prevails in the competition with the positive contribution of  $\rho_{22}E_2$  and leads to the destructive role the nonequilibrium effects that play in increasing the energy stored in the steady state of the ferromagnetic QB. From Fig. 7(d) we can see that, in the antiferromagnetic QB, the steady-state population components (component)  $\rho_{11}$ ,  $\rho_{22}$ ,  $\rho_{44}$  ( $\rho_{33}$ ) decrease (increase) with  $\Delta T > 0$ . Due to the fact that the eigenenergies  $E_2$  and  $E_4$  ( $E_1$  and  $E_3$ ) are positive (negative) for the chosen values of  $B_0 = 2$  and  $\Delta = 0.5$ , we find a positive contribution  $\rho_{11}$  but negative contribution for  $\rho_{22}$ ,  $\rho_{33}$ , and  $\rho_{44}$ . According to Fig. 7(d), applying a positive temperature gradient results in an increase in negative contribution of  $\rho_{22}E_2 + \rho_{33}E_3 + \rho_{44}E_4$

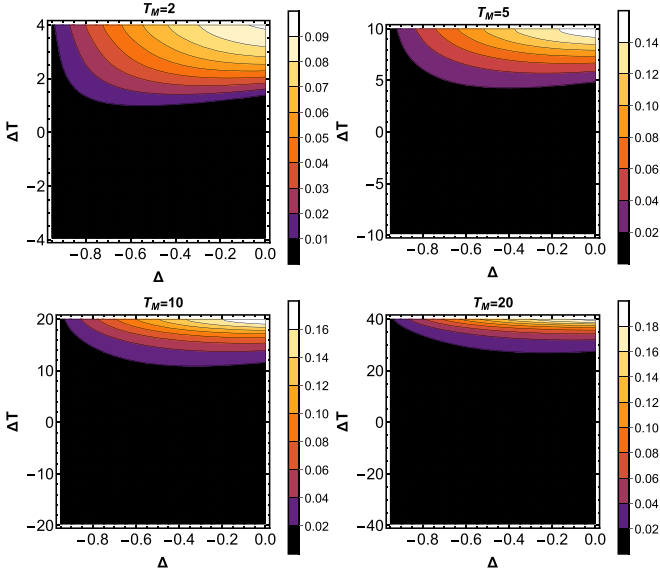


FIG. 8. NESS ergotropy  $W(\rho_{\text{NESS}})$  of the ferromagnetic spin-based QB versus  $\Delta$  and  $\Delta T$  for different values of  $T_M$  in the asymmetric spin-reservoir coupling setting. The chain anisotropy is set as  $B_0 = 2$ . All parameters of QB are in units of interspin coupling  $|J| = 1$ .

but positive contribution of  $\rho_{11}E_1$  to the stored energy in the steady state of the antiferromagnetic BQ.

#### IV. EXTRACTING ERGOTROPY FROM THE NONEQUILIBRIUM STEADY STATE OF THE TWO-SPIN FERROMAGNETIC AND ANTIFERROMAGNETIC XXZ QUANTUM BATTERIES

It is well known that, when an isolated system being in a state  $\rho = \sum_i r_i |r_i\rangle\langle r_i|$  evolves unitarily under a certain Hamiltonian  $H = \sum_{i=1} \varepsilon_i |\varepsilon_i\rangle\langle \varepsilon_i|$ , its internal energy does not change over time. However, the internal energy can be lowered by properly designed coupling with an external agent represented by an appropriate time-dependent potential  $V(t)$ . Such a potential is switched on during a certain time interval  $[0, T]$  and causes the Hamiltonian of the system to change periodically in the given time interval. When the system evolves under the Hamiltonian  $H_{\text{eff}} = H + V(t)$ , its dynamics are governed by the unitary time evolution operator  $U(T) = \mathcal{T} \exp\{-i \int_0^T dt [H + V(t)]\}$  for one period  $T$ , where  $\mathcal{T}$  denotes the time-ordering operator. After the period  $T$ , the system evolves into  $U(T)\rho U^\dagger(T)$ , and the amount of work that can be extracted via this unitary cyclic process is given by  $\text{Tr}(\rho H) - \text{Tr}(U\rho U^\dagger H)$ . By choosing the optimal unitary cyclic process, through appropriate designing of the time-dependent potential  $V(t)$ , it is possible to optimize the work extraction. The maximum amount of extractable work is called ergotropy [14] and is given by

$$W(\rho) = \text{Tr}(\rho H) - \min \text{Tr}(U\rho U^\dagger H), \quad (16)$$

where the minimization runs over all possible unitary operators that can extract work. The unitary operator  $U_{\text{min}}$  which achieves the maximum work, transforms  $\rho$  into a passive state  $\rho_p = \sum_k r_k |\varepsilon_k\rangle\langle \varepsilon_k|$  with decreasing populations  $r_k > r_{k+1}$  so

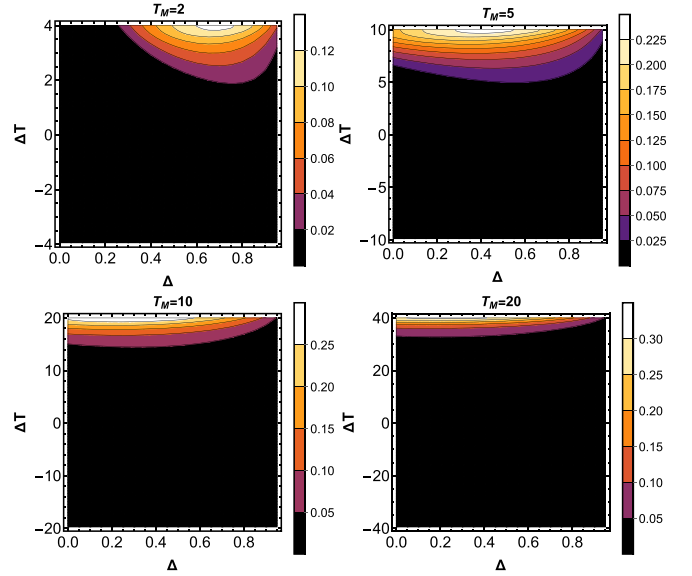


FIG. 9. NESS ergotropy  $W(\rho_{\text{NESS}})$  of the antiferromagnetic spin-based QB versus  $\Delta$  and  $\Delta T$  for different values of  $T_M$  in the asymmetric spin-reservoir coupling setting. The chain anisotropy is set as  $B_0 = 2$ . All parameters are in units of interspin coupling  $|J| = 1$ .

that work can no longer be extracted from this state cyclically [50–53]. By considering eigenvectors of  $H$  and  $\rho$ , the unitary operator  $U_{\text{min}}$  can be constructed as  $U_{\text{min}} = \sum_i |\varepsilon_i\rangle\langle r_i|$  and when inserted in Eq. (16) gives the following expression for the ergotropy

$$W(\rho) = \sum_{i,j} r_j \varepsilon_i (| \langle r_j | \varepsilon_i \rangle |^2 - \delta_{ij}), \quad (17)$$

which is zero for all passive states. It is worth noting that work can always be extracted from passive states by means of some collective process and thermal operations [8,11,40,54,55]. Within the family of passive states, thermal states are the only completely passive states from which no work could be extracted by means some collective process [56–59].

In the previous section we found that the asymmetric couplings of the QB to the thermal reservoirs induce NESS distributions of populations, where the ordering of populations changes as the positive temperature gradient increases. These results potentially suggest the possibility of activation of Gibbsian states with the aid of the inherent asymmetry. In Appendix A we have mathematically shown that, in the symmetric coupling setting the spin-chain QB initiated in the separable state  $|\Phi_1\rangle$  is passive and therefore work cannot be extracted from it by any unitary process. Now in this section we investigate the possibility of extraction of work from the NESS of ferromagnetic and antiferromagnetic spin-chain QBs in the asymmetric coupling setting. Figures 8 and 9 depict the NESS ergotropy of, respectively, the ferromagnetic and antiferromagnetic spin-chain QBs versus chain anisotropy  $\Delta$  and temperature gradient  $\Delta T$  for different  $T_M$  in the asymmetric spin-reservoir coupling setting. Obviously, the stored energy in the steady state of both ferromagnetic and antiferromagnetic spin-chain QB can be extracted by unitary processes, at the positive temperature bias. As can be seen,

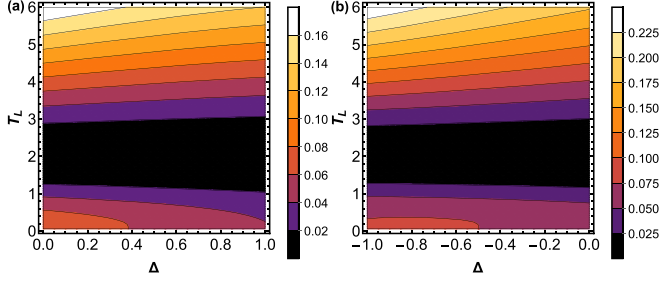


FIG. 10. NESS energy of (a) the antiferromagnetic and (b) the ferromagnetic  $XXZ$  QB versus  $\Delta$  and  $T_L$  in the symmetric coupling settings ( $\varepsilon = 0$ ). The magnetic field and inverse temperature of the reference heat reservoir are set as  $B_0 = 2$  and  $\beta_{\text{eq}} = 1/T_{\text{eq}} = 1/T_R = 0.5$ , respectively. All parameters of QB are in units of interspin coupling  $|J| = 1$ .

the maximum amount of work is extracted at  $\Delta T = 2T_M$ . Moreover, regardless of the ferromagnetic or antiferromagnetic properties of QB, ergotropy increases with the mean temperature of reservoirs  $T_M$ . More interestingly, comparing Fig. 5 (6) with Fig. 8 (9) indicates, although the steady-state stored energy of a ferromagnetic QB is more than that of the antiferromagnetic one, more energy can be extracted from the antiferromagnetic QB compared with the ferromagnetic QB.

It should be noted that our further calculations (not shown here) illustrate that, without the collective dissipation included in the model by introducing  $\mathcal{L}_L^{(1,2)}(\rho)$  in the master equation (10b), work cannot be extracted from NESS even in the presence of the inherent asymmetry. In other words, it is the collective dissipation which activates the NESS of the battery at the positive bias. Without the collective dissipation, the emission and absorption rates  $\gamma_{ij}^{(R,e)}$  and  $\gamma_{ij}^{(R,a)}$  given in (12a) and (B12) remain unchanged, while the emission and absorption rates  $\gamma_{ij}^{(L,e)}$  and  $\gamma_{ij}^{(L,a)}$  associated with the left reservoir are reduced to

$$\gamma_{ij}^{(L,e)} = 2\kappa\omega_{ij}[1 + n_L(\omega_{ij})], \quad \gamma_{ij}^{(L,a)} = 2\kappa\omega_{ij}n_L(\omega_{ij}). \quad (18)$$

With this in mind, passivity of the NESS without the collective dissipation can be proved analytically by a method similar to that used to prove its passivity in Appendix A for the case  $\varepsilon = 0$ .

Finally, it is needed to remark that some part of the total energy stored in the passive state of a QB can always be extracted through a nonunitary process under which the passive state is transformed to the Gibbsian thermal state  $\rho_{\text{eq}} = e^{-\beta_{\text{eq}} H_B} / \text{Tr}[e^{-\beta_{\text{eq}} H_B}]$ , in thermal contact with a reference heat reservoir at inverse temperature  $\beta_{\text{eq}}$ . The maximum extractable energy, under this thermalization process, is called exergy [55] quantified by the variation of the free energy [60–62] as

$$\sum_{\text{ex}} = \mathcal{F}(\rho_p) - \mathcal{F}(\rho_{\text{eq}}), \quad (19)$$

where  $\mathcal{F}(\rho_p) = \text{Tr}[H_B \rho_p] - \beta_{\text{eq}}^{-1} S(\rho_p)$  is the nonequilibrium Helmholtz free energy stored in the passive state with the von Neumann entropy  $S(\rho_p) = -\text{Tr}[\rho_p \ln \rho_p]$  [similarly for  $\mathcal{F}(\rho_{\text{eq}})$ ]. From the energy storage point of view,  $\sum_{\text{ex}}$  can be used to quantify the amount of usable energy stored in the passive state of an open QB that is charged within a thermal chamber at inverse temperature  $\beta_{\text{eq}}$  by a classical field [36]. For the passive steady state  $\rho_{\text{NESS}}$  at hand, we calculate the exergy given in (19) numerically in Fig. 10. Here  $\sum_{\text{ex}}$  is plotted as a function of  $\Delta$  and  $T_L$  for  $T_{\text{eq}} = T_R$ . As expected, regardless of the ferromagnetic or antiferromagnetic properties of the  $XXZ$  QB,  $\sum_{\text{ex}}$  increases with temperature gradient. However, NESS exergy of the ferromagnetic  $XXZ$  QB is more than those of the antiferromagnetic  $XXZ$  QB. It is clear that NESS exergy of the antiferromagnetic QB increases as the chain anisotropy  $\Delta$  decreases, so that a more exergy is extracted for the special case  $\Delta = 0$  correspond to NESS exergy of the  $XX$  QB. As it is shown, NESS exergy of the ferromagnetic QB, however, exhibits completely different behaviors with the increase of  $\Delta$ . In this situation, more NESS exergy is extracted for  $\Delta = -1$ , which corresponds to NESS exergy of the  $XXX$  QB.

## V. CHARGING A THREE-SPIN ANTIFERROMAGNETIC $XXZ$ QUANTUM BATTERY AND EXTRACTING ERGOTROPY FROM ITS NONEQUILIBRIUM STEADY STATE

In this section we generalize the spin-based QB of Sec. II to a three-spin  $XXZ$  QB with nearest-neighbor interaction. This spin model is described by the Hamiltonian of the form

$$\mathbb{H}_B = \frac{1}{2} \left[ B_0 \sum_{i=1}^3 \sigma_z^{(i)} + J \sum_{i=1}^2 \sigma_x^{(i)} \sigma_x^{(i+1)} + J \sum_{i=1}^2 \sigma_y^{(i)} \sigma_y^{(i+1)} + \Delta \sum_{i=1}^2 \sigma_z^{(i)} \sigma_z^{(i+1)} \right]. \quad (20)$$

The eigenenergies and corresponding eigenbasis of  $\mathbb{H}_B$  in the three-qubit bare basis  $\{|1, 1, 1\rangle, |1, 1, 0\rangle, |1, 0, 1\rangle, |0, 1, 1\rangle, |1, 0, 0\rangle, |0, 1, 0\rangle, |0, 0, 1\rangle, |0, 0, 0\rangle\}$  are

$$|\Psi_1\rangle = \frac{1}{\sqrt{2}}[|0, 0, 1\rangle - |1, 0, 0\rangle], \quad E_1 = -\frac{B_0}{2}, \quad (21a)$$

$$|\Psi_2\rangle = \frac{1}{\sqrt{2}}[|0, 1, 1\rangle - |1, 1, 0\rangle], \quad E_2 = \frac{B_0}{2}, \quad (21b)$$

$$|\Psi_3\rangle = |0, 0, 0\rangle, \quad E_3 = \frac{1}{2}(2\Delta - 3B_0), \quad (21c)$$

$$|\Psi_4\rangle = |1, 1, 1\rangle, \quad E_4 = \frac{1}{2}(2\Delta + 3B_0), \quad (21d)$$

$$|\Psi_5\rangle = \frac{1}{\sqrt{\left(\frac{\Delta+\alpha}{J}\right)^2 + 8}} \left[ 2|1, 0, 0\rangle - \frac{\Delta+\alpha}{J}|0, 1, 0\rangle + 2|0, 0, 1\rangle \right], \quad \mathbb{E}_5 = -\frac{1}{2}(B_0 + \Delta + \alpha), \quad (21e)$$

$$|\Psi_6\rangle = \frac{1}{\sqrt{\left(\frac{\Delta+\alpha}{J}\right)^2 + 8}} \left[ 2|1, 1, 0\rangle - \frac{\Delta+\alpha}{J}|1, 0, 1\rangle + 2|0, 1, 1\rangle \right], \quad \mathbb{E}_6 = \frac{1}{2}(B_0 - \Delta - \alpha), \quad (21f)$$

$$|\Psi_7\rangle = \frac{1}{\sqrt{\left(\frac{\Delta-\alpha}{J}\right)^2 + 8}} \left[ 2|1, 0, 0\rangle - \frac{\Delta-\alpha}{J}|0, 1, 0\rangle + 2|0, 0, 1\rangle \right], \quad \mathbb{E}_7 = -\frac{1}{2}(B_0 + \Delta - \alpha), \quad (21g)$$

$$|\Psi_8\rangle = \frac{1}{\sqrt{\left(\frac{\Delta-\alpha}{J}\right)^2 + 8}} \left[ 2|1, 1, 0\rangle - \frac{\Delta-\alpha}{J}|1, 0, 1\rangle + 2|0, 1, 1\rangle \right], \quad \mathbb{E}_8 = \frac{1}{2}(B_0 - \Delta + \alpha), \quad (21h)$$

where  $\alpha = (\Delta^2 + 8J^2)^{1/2}$ . This spin-chain QB is charged via the NESS heat current resulting from the weak coupling of the end qubits to two different thermal reservoirs. As illustrated in the schematic diagram in Fig. 11, the end qubits can be coupled to the reservoirs in two symmetrical coupling and asymmetrical coupling configurations. To establish the symmetrical coupling and asymmetrical coupling configurations we place a coupling switch between one end of the chain and one of the reservoirs. When the switch is off, the qubit 1 connects to reservoir  $\mathcal{R}_L$  with temperature  $T_L$  and the qubit 3 connects to the right reservoir  $\mathcal{R}_R$  with the temperature  $T_R$ . In this situation the QB coupled to the thermal reservoirs in a symmetric configuration. However, when the switch is flipped on, the QB is coupled to the reservoirs in an asymmetric configuration wherein qubit 3 is coupled to both reservoirs, whereas the qubit 1 is coupled to just the left reservoir. The dissipative interaction between the QB and harmonic oscillators of the left and right reservoirs is governed by the following Hamiltonian:

$$\mathbb{H}_{B-\text{res}} = \sum_j \lambda_j^{(L)} (\sigma_x^{(1)} + \varepsilon \sigma_x^{(3)}) (a_j^\dagger + a_j) + \lambda_j^{(R)} \sigma_x^{(3)} (b_j^\dagger + b_j), \quad (22)$$

where  $\lambda_j^{(L)}$  ( $\lambda_j^{(R)}$ ) are the dissipative interaction strengths between the QB and the  $j$ th oscillator of the left (right) reservoir with frequencies  $\omega_j^{(L)}$  ( $\omega_j^{(R)}$ ). In the weak-coupling regime, under the Born-Markov approximation, the master equation for the reduced density matrix of the chain reads

$$\dot{\rho}(t) = -i[\mathbb{H}_B, \rho(t)] + \mathcal{L}_L^{(1)}(\rho) + \mathcal{L}_R^{(3)}(\rho) + \varepsilon(\mathcal{L}_L^{(3)}(\rho) + \mathcal{L}_L^{(1,3)}(\rho)), \quad (23)$$

where the operator  $\mathcal{L}_v^{(k)}(\rho)$  represents dissipation due to the qubit  $k$  coupled individually to the reservoir  $\mathcal{R}_v$  and takes the form

$$\begin{aligned} \mathcal{L}_v^{(k)}(\rho) = & \sum_{\omega>0} \mathcal{J}_v(\omega) [1 + n_v(\omega)] \left[ \mathbb{V}^{(k)}(\omega) \rho(t) \mathbb{V}^{(k)\dagger}(\omega) - \frac{1}{2} \{ \mathbb{V}^{(k)\dagger}(\omega) \mathbb{V}^{(k)}(\omega), \rho(t) \} \right] \\ & + \sum_{\omega>0} \mathcal{J}_v(\omega) n_v(\omega) \left[ \mathbb{V}^{(k)\dagger}(\omega) \rho(t) \mathbb{V}^{(k)}(\omega) - \frac{1}{2} \{ \mathbb{V}^{(k)}(\omega) \mathbb{V}^{(k)\dagger}(\omega), \rho(t) \} \right], \end{aligned} \quad (24)$$

while  $\mathcal{L}_L^{(1,3)}(\rho)$  represents the collective dissipation due to the qubits 1 and 3 commonly coupled to the left reservoir has the form

$$\begin{aligned} \mathcal{L}_L^{(1,3)}(\rho) = & \sum_{\omega>0} \mathcal{J}_L(\omega) [1 + n_L(\omega)] \left[ \mathbb{V}^{(1)}(\omega) \rho(t) \mathbb{V}^{(3)\dagger}(\omega) - \frac{1}{2} \{ \mathbb{V}^{(3)\dagger}(\omega) \mathbb{V}^{(1)}(\omega), \rho(t) \} \right] \\ & + \sum_{\omega>0} \mathcal{J}_L(\omega) n_L(\omega) \left[ \mathbb{V}^{(1)\dagger}(\omega) \rho(t) \mathbb{V}^{(3)}(\omega) - \frac{1}{2} \{ \mathbb{V}^{(3)}(\omega) \mathbb{V}^{(1)\dagger}(\omega), \rho(t) \} \right] \\ & + \sum_{\omega>0} \mathcal{J}_L(\omega) [1 + n_L(\omega)] \left[ \mathbb{V}^{(3)}(\omega) \rho(t) \mathbb{V}^{(1)\dagger}(\omega) - \frac{1}{2} \{ \mathbb{V}^{(1)\dagger}(\omega) \mathbb{V}^{(3)}(\omega), \rho(t) \} \right] \\ & + \sum_{\omega>0} \mathcal{J}_L(\omega) n_L(\omega) \left[ \mathbb{V}^{(3)\dagger}(\omega) \rho(t) \mathbb{V}^{(1)}(\omega) - \frac{1}{2} \{ \mathbb{V}^{(1)}(\omega) \mathbb{V}^{(3)\dagger}(\omega), \rho(t) \} \right]. \end{aligned} \quad (25)$$

In the above equations,  $\mathbb{V}^{(k)}(\omega) = \sum_{\mathbb{E}_i - \mathbb{E}_j = \omega > 0} |\Psi_j\rangle \langle \Psi_j | \sigma_x^{(k)} | \Psi_i\rangle \langle \Psi_i |$  is the transition operator corresponding to the transition between two eigenbasis  $|\Psi_i\rangle$  and  $|\Psi_j\rangle$ .

Now, with the assumed Ohmic type of spectral density, and by substituting Eqs. (24), (25) and (20) into Eq. (23), the master equation can be reexpressed as

$$\begin{aligned} \dot{\rho}(t) = & -i[\mathbb{H}_B, \rho(t)] + \sum_{v=L,R} [\gamma_{13}^{(v,e)} L_{\tau_{31}} + \gamma_{13}^{(v,a)} L_{\tau_{13}} + \gamma_{61}^{(v,e)} L_{\tau_{16}} + \gamma_{61}^{(v,a)} L_{\tau_{61}} + \gamma_{81}^{(v,e)} L_{\tau_{18}} + \gamma_{81}^{(v,a)} L_{\tau_{81}} + \gamma_{42}^{(v,e)} L_{\tau_{24}} \\ & + \gamma_{42}^{(v,a)} L_{\tau_{42}} + \gamma_{25}^{(v,e)} L_{\tau_{52}} + \gamma_{25}^{(v,a)} L_{\tau_{25}} + \gamma_{27}^{(v,e)} L_{\tau_{72}} + \gamma_{27}^{(v,a)} L_{\tau_{27}} + \gamma_{46}^{(v,e)} L_{\tau_{64}} + \gamma_{46}^{(v,a)} L_{\tau_{46}} + \gamma_{65}^{(v,e)} L_{\tau_{56}} \\ & + \gamma_{65}^{(v,a)} L_{\tau_{65}} + \gamma_{67}^{(v,e)} L_{\tau_{76}} + \gamma_{67}^{(v,a)} L_{\tau_{67}} + \gamma_{85}^{(v,e)} L_{\tau_{58}} + \gamma_{85}^{(v,a)} L_{\tau_{85}} + \gamma_{87}^{(v,e)} L_{\tau_{78}} + \gamma_{87}^{(v,a)} L_{\tau_{87}}], \end{aligned} \quad (26)$$

where  $\tau_{ij} = |\Psi_i\rangle\langle\Psi_j|$ ,  $L_X = X\rho X^\dagger - \frac{1}{2}\{\rho, X^\dagger X\}$ . The emission and absorption rates associated with interaction between the QB and right reservoir are of the form

$$\gamma_{ij}^{(R,e)} = \frac{1}{2}\kappa\omega_{ij}[1 + n_R(\omega_{ij})], \quad \gamma_{ij}^{(R,a)} = \frac{1}{2}\kappa\omega_{ij}n_R(\omega_{ij}), \quad (27)$$

The emission and absorption rates associated with interaction between the QB and left reservoir are given in Appendix B.

The master equation (26) can be represented in the energy basis. In this representation, dynamical equations for the density-matrix elements are given in Appendix C. With these dynamical equations, the elements of steady-state density matrix can be obtained by solving the equation  $d\rho/dt = 0$ . The explicit form of the steady-state density matrix elements are relatively complex and so we not report them here.

In what follows, we explore the nonequilibrium effects on the steady-state ergotropy as well as stored energy in the steady state of the three-qubit  $XXZ$  spin-chain QB. Here we restrict to charging processes in which the battery is initially in  $|\Psi_3\rangle = |0, 0, 0\rangle$ . Therefore, in order to inject energy to the battery, the system parameters have to be set  $B > |\frac{3\Delta + \alpha}{2}|$ .

In Fig. 12 we plot the NESS stored energy  $\Delta E_B(\infty)$  and NESS ergotropy  $W(\infty)$  of a three-spin antiferromagnetic  $XXZ$  QB as a function of the chain anisotropy  $\Delta$  for different values of mean temperature  $T_M$  and positive temperature bias  $\Delta T$  in the both symmetric and asymmetric coupling settings. The NESS stored energy, as shown in Fig. 12(a), in general displays monotonic behaviors with respect to  $\Delta$  in both the

symmetric and asymmetric coupling configurations; at low mean temperatures,  $\Delta E_B(\infty)$  does not change significantly with  $\Delta$ , while at enough mean temperature it decreases with  $\Delta$ . Figure 12(a) shows that, similar to the case of two-qubit spin-chain QB, nonequilibrium effects play constructive role in enhancing the NESS stored energy in both the symmetric and asymmetric coupling configurations. Comparing the NESS stored energy in the symmetrical coupling configuration with that in the asymmetrical coupling configuration, we find that more energy is stored in the steady state of QB when it is asymmetrically coupled to the thermal reservoirs.

Figure 12(b) reveals that the stored energy in the steady state of the three-qubit  $XXZ$  spin-chain QB can be extracted by unitary processes only when the coupling switch between the qubit 3 and the left reservoir is on ( $\varepsilon = 1$ ). As can be seen, in this case, the nonequilibrium effects play constructive role in enhancing the NESS ergotropy. More specifically, more energy can be extracted from the steady state of QB when the temperature gradient is increased to  $\Delta T = 2T_M$ .

## VI. OUTLOOK AND SUMMARY

To summarize, we proposed a two-qubit  $XXZ$  spin-chain QB coupled weakly to two independent Ohmic thermal reservoirs. We considered two different coupling settings, a symmetric configuration wherein each qubit interacts with an individual reservoir, and an asymmetric configuration wherein one qubit interacts with both reservoirs, whereas the another qubit is coupled to just one of them. This QB could be implemented in a circuit QED system [42], where an anharmonic circuit with Josephson junctions, as a four-level transmon qubit, is coupled to two thermal reservoir circuits.

By assuming that both qubits are initiated in their ground states, we showed that the QB can be charged via the nonequilibrium steady-state (NESS) heat current in a weak

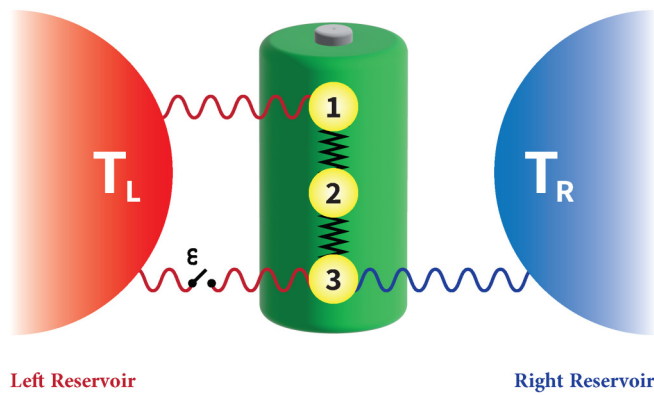


FIG. 11. The schematic diagram of the three-spin  $XXZ$  spin-chain QB with two end qubits 1 and 3 interacting with a nonequilibrium environment consists of left and right reservoirs. The key  $\varepsilon$  is used to switch on and off the coupling between the end qubit 3 and the left reservoir, which allows us to control chain-reservoir coupling asymmetry.

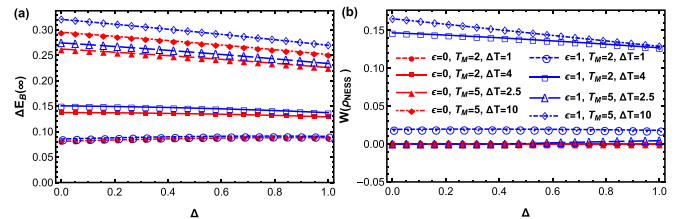


FIG. 12. (a) The NESS stored energy  $\Delta E_B(\infty)$  and (b) the NESS ergotropy  $W(\rho_{\text{NESS}})$  of a three-spin antiferromagnetic  $XXZ$  QB versus  $\Delta$  for different values of  $T_M$  and  $\Delta T$  in the symmetric and asymmetric coupling settings. The chain anisotropy is set as  $B_0 = 5$ . All parameters of QB are in units of interspin coupling  $|J| = 1$ .

qubit-reservoir coupling regime. Our numerical results revealed, regardless the ferromagnetic or antiferromagnetic properties of chain, nonequilibrium effects of heat current play constructive role at low base temperature of the reservoirs, while they act destructively when the temperature is high enough. We found that the inherent asymmetry induced by the asymmetrically couplings of QB to the reservoirs, suppresses the destructive effects of heat current generated at large negative bias. Finally, we proved our main results of this paper, and showed that the two-qubit QB coupled symmetrically to two thermal reservoirs is passive, while asymmetric coupling of such QB to the thermal reservoirs brings it to a NESS from which it is possible to extract work through unitary cyclic processes, i.e., the QB can have nonzero ergotropy. We found that ergotropy is achievable at the positive temperature bias  $\Delta T > 0$ , and it can be significantly enhanced close to  $\Delta T = 2T_M$ .

To confirm the same conclusions are also applicable to the battery with more spins, we numerically discussed the case of antiferromagnetic  $XXZ$  spin-chain QB composed of three spins. We found that considering more spins does not change the conclusions.

Our results present a charging protocol to have an active QB, without need for further control. This charging protocol can be easily implemented in the circuit-QED setups where qubit-reservoir interaction is tuned through including some  $LC$  circuit band-pass filters between the qudit transmon and one of the thermal circuits. Here the asymmetry in the qudit-reservoir coupling can be modeled by inclusion some additional filters between the qudit transmon and the hot thermal circuit.

#### APPENDIX A: A MATHEMATICAL PROOF FOR THE PASSIVITY OF $\rho_{\text{NESS}}$ IN THE CASE OF $\varepsilon = 0$

Here we prove why  $\rho_{\text{NESS}}$  with components given in (13a)–(13d) is a passive state in the symmetric battery-reservoir coupling setting (i.e.,  $\varepsilon = 0$ ). In what follows, we first prove this for the antiferromagnetic battery ( $J > 0$  and  $\Delta > 0$ ).

Recall that in the limit we are working in ( $B > |J + \Delta|$ ), the eigenenergies of the antiferromagnetic battery satisfy the ordering  $E_2 > E_4 > E_3 > E_1$ . So to show that  $\rho_{\text{NESS}}$  is a passive state, we must prove that its components in the energy basis satisfy  $\rho_{11} > \rho_{33} > \rho_{44} > \rho_{22}$ . Depending on whether  $J < \Delta$  or  $\Delta < J$ , the transition frequencies  $\omega_{ij}$  satisfy the following inequality relations:

$$\omega_{23} > \omega_{24} > \omega_{41} > \omega_{31}, \quad J < \Delta, \quad (\text{A1})$$

$$\omega_{23} > \omega_{41} > \omega_{24} > \omega_{31}, \quad J > \Delta. \quad (\text{A2})$$

According to the above inequalities, we would have

$$\frac{1}{e^{\frac{\omega_{24}}{T_L} - 1}} + \frac{1}{e^{\frac{\omega_{24}}{T_R} - 1}} > \frac{1}{e^{\frac{\omega_{23}}{T_L} - 1}} + \frac{1}{e^{\frac{\omega_{23}}{T_R} - 1}}, \quad (\text{A3})$$

$$\frac{1}{e^{\frac{\omega_{31}}{T_L} - 1}} + \frac{1}{e^{\frac{\omega_{31}}{T_R} - 1}} > \frac{1}{e^{\frac{\omega_{41}}{T_L} - 1}} + \frac{1}{e^{\frac{\omega_{41}}{T_R} - 1}}. \quad (\text{A4})$$

Now, by multiplying both sides of the inequalities (A3) and (A4), respectively, by  $2\omega_{24}\omega_{23}$  and  $2\omega_{41}\omega_{31}$ , we

obtain

$$2\omega_{23}(\gamma_{24}^{(L,a)} + \gamma_{24}^{(R,a)}) > 2\omega_{24}(\gamma_{23}^{(L,a)} + \gamma_{23}^{(R,a)}), \quad (\text{A5})$$

$$2\omega_{41}(\gamma_{31}^{(L,a)} + \gamma_{31}^{(R,a)}) > 2\omega_{31}(\gamma_{41}^{(L,a)} + \gamma_{41}^{(R,a)}), \quad (\text{A6})$$

for  $\varepsilon = 0$ . Next, adding the positive terms  $(\gamma_{24}^{(L,a)} + \gamma_{24}^{(R,a)}) + (\gamma_{23}^{(L,a)} + \gamma_{23}^{(R,a)})$  and  $(\gamma_{31}^{(L,a)} + \gamma_{31}^{(R,a)}) + (\gamma_{41}^{(L,a)} + \gamma_{41}^{(R,a)})$ , respectively, in both sides of (A.5) and (A.6), implies the following results:

$$A_{24}E_{23} > A_{23}E_{24}, \quad (\text{A7})$$

$$A_{31}E_{41} > A_{41}E_{31}, \quad (\text{A8})$$

where we have used  $\gamma_{ij}^{(L,\varepsilon)} = \gamma_{ij}^{(L,a)} + \kappa\omega_{ij}/2$  which is a direct consequence of symmetric battery-reservoir coupling configuration. Now dividing the both sides of (A7) and (A8) respectively by  $(A_{23} + E_{31})(E_{23} + E_{24})$  and  $(A_{23} + E_{31})(A_{31} + A_{41})$  and adding the respective sides of the resulting inequalities, we get  $\eta_1 > \eta_2$ , and hence we obtain  $\rho_{33} > \rho_{44}$ .

On the other hand, From Eqs. (A1) and (A2), we conclude

$$\frac{1}{e^{\omega_{41}/T_\nu} - 1} > \frac{1}{e^{\omega_{23}/T_\nu} - 1}$$

( $\nu = L, R$ ). By replacing  $\nu$  with  $L$  and again with  $R$ , adding the respective sides of the resulting inequalities and using

$$n_L(\omega) = [e^{\frac{\omega}{T_L}} - 1]^{-1}, \quad n_R(\omega) = [e^{\frac{\omega}{T_R}} - 1]^{-1},$$

we obtain

$$n_L(\omega_{41}) + n_R(\omega_{41}) > n_L(\omega_{23}) + n_R(\omega_{23}). \quad (\text{A9})$$

Next, by multiplying both sides of the above inequality by  $2\omega_{41}\omega_{23}$  and using the Eq. (B12), we obtain

$$\frac{\omega_{23}}{A_{23}} > \frac{\omega_{41}}{A_{41}}. \quad (\text{A10})$$

Using the  $\gamma_{ij}^{(L,\varepsilon)} = \gamma_{ij}^{(L,a)} + \kappa\omega_{ij}/2$  which hold true only for  $\varepsilon = 0$ , we conclude that

$$E_{23}A_{41}E_{31} > A_{31}E_{41}A_{23}, \quad (\text{A11})$$

where we have used  $E_{31} > A_{31}$ . Multiplying the inequality  $E_{24} > A_{24}$  by

$$\frac{E_{23}A_{23}}{E_{23} + E_{24}} + \eta_2,$$

dividing inequality (A11) by  $A_{31} + A_{41}$ , adding the respective sides of the resulting inequalities, we obtain  $\eta_2(E_{23} + E_{24}) > \eta_1A_{23} + \eta_2A_{24}$ . Hence we get

$$\frac{\rho_{44}}{\rho_{22}} = \frac{\eta_2(E_{23} + E_{24})}{\eta_1A_{23} + \eta_2A_{24}} > 1. \quad (\text{A12})$$

Furthermore, in the limit we are working, the transition frequency  $\omega_{23}$  is less than  $\omega_{24} + \omega_{14}$ . It is then easy to see that the following inequality holds true for any  $T$ ,

$$\frac{e^{\frac{\omega_{24} + \omega_{14}}{T}} - 1}{e^{\frac{\omega_{23}}{T}} - 1} > 1. \quad (\text{A13})$$

Now by replacing  $T$  in the above inequality once with  $T_M$  and once with  $2T_M$ , we get the following inequalities

$$(e^{\frac{\omega_{24}}{T_M}} - 1)(e^{\frac{\omega_{41}}{T_M}} - 1) + (e^{\frac{\omega_{24}}{2T_M}} - 1) + (e^{\frac{\omega_{41}}{2T_M}} - 1) > e^{\frac{\omega_{23}}{T_M}} - 1, \quad (\text{A14})$$

$$(e^{\frac{\omega_{24}}{2T_M}} - 1)(e^{\frac{\omega_{41}}{2T_M}} - 1) + (e^{\frac{\omega_{24}}{T_M}} - 1) + (e^{\frac{\omega_{41}}{T_M}} - 1) > e^{\frac{\omega_{23}}{2T_M}} - 1. \quad (\text{A15})$$

Multiplying both sides of the inequalities (A14) and (A15) by  $1/2$  and using

$$n_{L(R)}(\omega) = [e^{\frac{\omega}{T_M \pm \Delta T/2}} - 1]^{-1},$$

we conclude that the following inequality holds true for  $\Delta T = 0$  as well as  $\Delta T = \pm 2T_M$ :

$$\begin{aligned} & \frac{2}{[n_L(\omega_{41}) + n_R(\omega_{41})][n_L(\omega_{24}) + n_R(\omega_{24})]} \\ & + \frac{1}{n_L(\omega_{41}) + n_R(\omega_{41})} + \frac{1}{n_L(\omega_{24}) + n_R(\omega_{24})} \\ & > \frac{1}{n_L(\omega_{23}) + n_R(\omega_{23})}. \end{aligned} \quad (\text{A16})$$

Since both sides of the inequality (A16) are strictly increasing (decreasing) functions on an interval  $\Delta T \in [-2T_M, 0]$  ( $\Delta T \in$

$[0, 2T_M]$ ), one can conclude that the inequality (A16) holds true for any  $\Delta T$  and therefore for any  $T$ .

Now, by multiplying the numerator as well as denominator of left (right) side of (A15) by  $\omega_{41}\omega_{24}$  ( $\omega_{23}$ ) one can obtain

$$\frac{2\omega_{41}\omega_{24}}{A_{41}A_{24}} + \frac{\omega_{41}}{A_{24}} + \frac{\omega_{24}}{A_{24}} > \frac{\omega_{23}}{A_{23}}, \quad (\text{A17})$$

which can be simplified to

$$\frac{E_{41} E_{24}}{A_{41} A_{24}} > \frac{E_{23}}{A_{23}}, \quad (\text{A18})$$

where we have used  $E_{ij} = A_{ij} + \omega_{ij}$ . Furthermore, by multiplying both sides of (A18) and the inequality  $E_{31} > A_{31}$ , respectively by  $A_{23}A_{41}A_{24}/(E_{23} + E_{24})$  and  $E_{41}A_{41}/(A_{31} + A_{41}) + \eta_1$ , then adding the respective sides of the resulting inequalities, we obtain  $\eta_2 E_{41} + \eta_1 E_{31} > \eta_1 (A_{31} + A_{41})$  and hence we get  $\rho_{11} > \rho_{33}$ .

For the ferromagnetic case ( $J < 0$  and  $\Delta < 0$ ), one can in a similar manner prove that  $E_i > E_j$  implies  $\rho_{ii} \leq \rho_{jj} \forall i, j$ , so  $\rho_{\text{NESS}}$  associated with the ferromagnetic QB is a passive state in the symmetric battery-reservoir coupling setting.

## APPENDIX B: EXPRESSIONS OF $\gamma_{ij}^{(L,e)}$ AND $\gamma_{ij}^{(L,a)}$ GIVEN IN EQ. (26)

The emission and absorption rates, thanks to the interaction of the QB with the left reservoir given in Eq. (26) have the following expressions:

$$\gamma_{13}^{(L,e)} = \frac{1}{2}\kappa\omega_{13}(\varepsilon - 1)^2[1 + n_L(\omega_{13})], \quad \gamma_{13}^{(L,a)} = \frac{1}{2}\kappa\omega_{13}(\varepsilon - 1)^2 n_L(\omega_{13}), \quad (\text{B1})$$

$$\gamma_{61}^{(L,e)} = \frac{1}{2}\kappa\omega_{61}(\varepsilon - 1)^2 \left(\frac{\Delta + \alpha}{J}\right)^2 x^2 [1 + n_L(\omega_{61})], \quad \gamma_{61}^{(L,a)} = \frac{1}{2}\kappa\omega_{61}(\varepsilon - 1)^2 \left(\frac{\Delta + \alpha}{J}\right)^2 x^2 n_L(\omega_{61}), \quad (\text{B2})$$

$$\gamma_{81}^{(L,e)} = \frac{1}{2}\kappa\omega_{81}(\varepsilon - 1)^2 \left(\frac{\Delta - \alpha}{J}\right)^2 y^2 [1 + n_L(\omega_{61})], \quad \gamma_{81}^{(L,a)} = \frac{1}{2}\kappa\omega_{81}(\varepsilon - 1)^2 \left(\frac{\Delta - \alpha}{J}\right)^2 y^2 n_L(\omega_{81}), \quad (\text{B3})$$

$$\gamma_{42}^{(L,e)} = \frac{1}{2}\kappa\omega_{42}(\varepsilon - 1)^2 [1 + n_L(\omega_{42})], \quad \gamma_{42}^{(L,a)} = \frac{1}{2}\kappa\omega_{42}(\varepsilon - 1)^2 n_L(\omega_{42}), \quad (\text{B4})$$

$$\gamma_{25}^{(L,e)} = \frac{1}{2}\kappa\omega_{25}(\varepsilon - 1)^2 \left(\frac{\Delta + \alpha}{J}\right)^2 x^2 [1 + n_L(\omega_{25})], \quad \gamma_{25}^{(L,a)} = \frac{1}{2}\kappa\omega_{25}(\varepsilon - 1)^2 \left(\frac{\Delta + \alpha}{J}\right)^2 x^2 n_L(\omega_{25}), \quad (\text{B5})$$

$$\gamma_{27}^{(L,e)} = \frac{1}{2}\kappa\omega_{27}(\varepsilon - 1)^2 \left(\frac{\Delta - \alpha}{J}\right)^2 y^2 [1 + n_L(\omega_{27})], \quad \gamma_{27}^{(L,a)} = \frac{1}{2}\kappa\omega_{27}(\varepsilon - 1)^2 \left(\frac{\Delta - \alpha}{J}\right)^2 y^2 n_L(\omega_{27}), \quad (\text{B6})$$

$$\gamma_{46}^{(L,e)} = 4\kappa\omega_{46}(\varepsilon + 1)^2 x^2 [1 + n_L(\omega_{46})], \quad \gamma_{46}^{(L,a)} = 4\kappa\omega_{46}(\varepsilon + 1)^2 x^2 n_L(\omega_{46}), \quad (\text{B7})$$

$$\gamma_{48}^{(L,e)} = 4\kappa\omega_{48}(\varepsilon + 1)^2 y^2 [1 + n_L(\omega_{48})], \quad \gamma_{48}^{(L,a)} = 4\kappa\omega_{48}(\varepsilon + 1)^2 y^2 n_L(\omega_{48}), \quad (\text{B8})$$

$$\gamma_{65}^{(L,e)} = 16\kappa\omega_{65}(\varepsilon + 1)^2 \left(\frac{\Delta + \alpha}{J}\right)^2 x^2 [1 + n_L(\omega_{65})], \quad \gamma_{65}^{(L,a)} = 16\kappa\omega_{65}(\varepsilon + 1)^2 \left(\frac{\Delta + \alpha}{J}\right)^2 x^2 n_L(\omega_{65}), \quad (\text{B9})$$

$$\gamma_{67}^{(L,e)} = 16\kappa\omega_{67}(\varepsilon + 1)^2 \left(\frac{\Delta}{J}\right)^2 x^2 y^2 [1 + n_L(\omega_{67})], \quad \gamma_{67}^{(L,a)} = 16\kappa\omega_{67}(\varepsilon + 1)^2 \left(\frac{\Delta}{J}\right)^2 x^2 y^2 n_L(\omega_{67}), \quad (\text{B10})$$

$$\gamma_{85}^{(L,e)} = 16\kappa\omega_{85}(\varepsilon + 1)^2 \left(\frac{\Delta}{J}\right)^2 x^2 y^2 [1 + n_L(\omega_{85})], \quad \gamma_{85}^{(L,a)} = 16\kappa\omega_{85}(\varepsilon + 1)^2 \left(\frac{\Delta}{J}\right)^2 x^2 y^2 n_L(\omega_{85}), \quad (\text{B11})$$

$$\gamma_{87}^{(L,e)} = 16\kappa\omega_{87}(\varepsilon + 1)^2 \left(\frac{\Delta - \alpha}{J}\right)^2 y^4 [1 + n_L(\omega_{87})], \quad \gamma_{87}^{(L,a)} = 16\kappa\omega_{87}(\varepsilon + 1)^2 \left(\frac{\Delta - \alpha}{J}\right)^2 y^4 n_L(\omega_{87}), \quad (\text{B12})$$

with  $x = [(\frac{\Delta+\alpha}{J})^2 + 8]^{-\frac{1}{2}}$  and  $y = [(\frac{\Delta-\alpha}{J})^2 + 8]^{-\frac{1}{2}}$ .

### APPENDIX C: DYNAMICAL MASTER EQUATION (26) IN THE ENERGY-BASIS REPRESENTATION

To obtain the steady-state solution of the three-spin  $XXZ$  QB, first, we rewrite the master equation (26) in the energy basis representation and derive a set of 64 dynamical equations for the density-matrix elements. Eight of them are coupled differential equations for diagonal elements, decoupled from nondiagonal ones, that describe the evolution of the populations of the eight energy levels,  $\{\rho_{ii}\}$  ( $i = 1, 2, \dots, 8$ ), and the rest are decoupled differential equations for nondiagonal elements that describe coherence between the eight energy levels  $\{\rho_{ij}\}$  ( $i \neq j = 1, 2, \dots, 8$ ). The differential equations for the diagonal elements are

$$\dot{\rho}_{11} = \sum_{v=L,R} [\gamma_{13}^{(v,a)} \rho_{33} + \gamma_{61}^{(v,e)} \rho_{66} + \gamma_{81}^{(v,e)} \rho_{88} - (\gamma_{13}^{(v,e)} + \gamma_{61}^{(v,a)} + \gamma_{81}^{(v,a)}) \rho_{11}], \quad (\text{C1})$$

$$\dot{\rho}_{22} = \sum_{v=L,R} [\gamma_{42}^{(v,e)} \rho_{44} + \gamma_{25}^{(v,a)} \rho_{55} + \gamma_{27}^{(v,a)} \rho_{77} - (\gamma_{42}^{(v,a)} + \gamma_{25}^{(v,e)} + \gamma_{27}^{(v,e)}) \rho_{22}], \quad (\text{C2})$$

$$\dot{\rho}_{33} = \sum_{v=L,R} [\gamma_{13}^{(v,e)} \rho_{11} - \gamma_{13}^{(v,a)} \rho_{33}], \quad (\text{C3})$$

$$\dot{\rho}_{44} = \sum_{v=L,R} [\gamma_{42}^{(v,a)} \rho_{22} + \gamma_{46}^{(v,a)} \rho_{66} + \gamma_{48}^{(v,a)} \rho_{88} - (\gamma_{42}^{(v,e)} + \gamma_{46}^{(v,e)} + \gamma_{48}^{(v,e)}) \rho_{44}], \quad (\text{C4})$$

$$\dot{\rho}_{55} = \sum_{v=L,R} [\gamma_{25}^{(v,e)} \rho_{22} + \gamma_{65}^{(v,e)} \rho_{66} + \gamma_{85}^{(v,e)} \rho_{88} - (\gamma_{25}^{(v,a)} + \gamma_{65}^{(v,a)} + \gamma_{85}^{(v,a)}) \rho_{55}], \quad (\text{C5})$$

$$\dot{\rho}_{66} = \sum_{v=L,R} [\gamma_{61}^{(v,a)} \rho_{11} + \gamma_{46}^{(v,e)} \rho_{44} + \gamma_{65}^{(v,a)} \rho_{55} + \gamma_{67}^{(v,a)} \rho_{77} - (\gamma_{61}^{(v,e)} + \gamma_{46}^{(v,a)} + \gamma_{65}^{(v,e)} + \gamma_{67}^{(v,e)}) \rho_{66}], \quad (\text{C6})$$

$$\dot{\rho}_{77} = \sum_{v=L,R} [\gamma_{27}^{(v,e)} \rho_{22} + \gamma_{67}^{(v,e)} \rho_{66} + \gamma_{87}^{(v,e)} \rho_{88} - (\gamma_{27}^{(v,a)} + \gamma_{67}^{(v,a)} + \gamma_{87}^{(v,a)}) \rho_{77}], \quad (\text{C7})$$

$$\dot{\rho}_{88} = \sum_{v=L,R} [\gamma_{81}^{(v,a)} \rho_{11} + \gamma_{48}^{(v,e)} \rho_{44} + \gamma_{85}^{(v,a)} \rho_{55} + \gamma_{87}^{(v,a)} \rho_{77} - (\gamma_{81}^{(v,e)} + \gamma_{48}^{(v,a)} + \gamma_{85}^{(v,e)} + \gamma_{87}^{(v,e)}) \rho_{88}]. \quad (\text{C8})$$

Moreover, we find that the differential equations for the nondiagonal elements have exponential solutions which become zero in the steady-state limit ( $t \rightarrow \infty$ ). Therefore, all the nondiagonal elements of the density matrix are irrelevant for the steady-state performance of the QB.

Writing the above set of equations (C1)–(C8) in vector-matrix form as  $\frac{d}{dt}|\rho\rangle = \mathcal{M}|\rho\rangle$ , with  $|\rho\rangle = (\rho_{11}, \rho_{22}, \dots, \rho_{77}, 1 - \sum_{i=1}^7 \rho_{ii})^T$ , we obtain uniquely the relevant steady-state density matrix elements by obtaining the kernel of  $\mathcal{M}$ , that is,  $\mathcal{M}|\rho_{\text{NESS}}\rangle = 0$ .

- 
- [1] R. Alicki and M. Fannes, Entanglement boost for extractable work from ensembles of quantum batteries, *Phys. Rev. E* **87**, 042123 (2013).
- [2] D. Farina, G. M. Andolina, A. Mari, M. Polini, and V. Giovannetti, Charger-mediated energy transfer for quantum batteries: An open system approach, *Phys. Rev. B* **99**, 035421 (2019).
- [3] Y.-Y. Zhang, T.-R. Yang, L. Fu, and X. Wang, Powerful harmonic charging in a quantum battery, *Phys. Rev. E* **99**, 052106 (2019).
- [4] L. Fusco, M. Paternostro, and G. De Chiara, *Phys. Rev. E* **94**, 052122 (2016).
- [5] R. R. Rodríguez, B. Ahmadi, P. Mazurek, S. Barzanjeh, R. Alicki, and P. Horodecki, Catalysis in charging quantum batteries, *Phys. Rev. A* **107**, 042419 (2023).
- [6] J. Carrasco, J. R. Maze, C. Hermann-Avigliano, and F. Barra, Collective enhancement in dissipative quantum batteries, *Phys. Rev. E* **105**, 064119 (2022).
- [7] M. Gumberidze, M. Kolár, and R. Filip, Measurement induced synthesis of coherent quantum batteries, *Sci. Rep.* **9**, 19628 (2019).
- [8] D. Ferraro, M. Campisi, G. M. Andolina, V. Pellegrini, and M. Polini, High-power collective charging of a solid-state quantum battery, *Phys. Rev. Lett.* **120**, 117702 (2018).
- [9] V. Shaghghi, V. Singh, G. Benenti, and D. Rosa, Micromasers as quantum batteries, *Quantum Sci. Technol.* **7**, 04LT01 (2022).
- [10] M. B. Arjmandi, A. Shokri, E. Faizi, and H. Mohammadi, Performance of quantum batteries with correlated and uncorrelated chargers, *Phys. Rev. A* **106**, 062609 (2022).
- [11] F. Campaioli, F. A. Pollock, F. C. Binder, L. Céleri, J. Goold, S. Vinjanampathy, and K. Modi, Enhancing the charging power of quantum batteries, *Phys. Rev. Lett.* **118**, 150601 (2017).
- [12] S. Julià-Farré, T. Salamon, A. Riera, M. N. Bera, and M. Lewenstein, Bounds on the capacity and power of quantum batteries, *Phys. Rev. Res.* **2**, 023113 (2020).

- [13] A. Delmonte, A. Crescente, M. Carrega, D. Ferraro, and M. Sassetti, Characterization of a two-photon quantum battery: Initial conditions, stability and work extraction, *Entropy* **23**, 612 (2021).
- [14] A. E. Allahverdyan, R. Balian, and T. M. Nieuwenhuizen, Maximal work extraction from finite quantum systems, *Europhys. Lett.* **67**, 565 (2004).
- [15] D. Šafránek, D. Rosa, and F. Binder, Work extraction from unknown quantum sources, *Phys. Rev. Lett.* **130**, 210401 (2023).
- [16] F. Centrone, L. Mancino, and M. Paternostro, Charging batteries with quantum squeezing, *Phys. Rev. A* **108**, 052213 (2023).
- [17] C. Rodríguez, D. Rosa, and J. Olle, Artificial intelligence discovery of a charging protocol in a micromaser quantum battery, *Phys. Rev. A* **108**, 042618 (2023).
- [18] D. Rosa, D. Rossini, G. M. Andolina, M. Polinib, and M. Carregad, Ultra-stable charging of fast-scrambling syk quantum batteries, *J. High Energy Phys.* **11** (2020) 067.
- [19] B. Mojaveri, R. J. Bahrbeig, M. A. Fasihi, and S. Babanzadeh, Enhancing the performance of an open quantum battery by adjusting its velocity, *Sci. Rep.* **13**, 19827 (2023).
- [20] M. T. Mitchison, J. Goold, and J. Prior, Charging a quantum battery with linear feedback control, *Quantum* **5**, 500 (2021).
- [21] Y. Yao and X. Q. Shao, Optimal charging of open spin-chain quantum batteries via homodyne-based feedback control, *Phys. Rev. E* **106**, 014138 (2022).
- [22] S. Borisenok, Ergotropy of quantum battery controlled via target attractor feedback, *IOSR J. Appl. Phys.* **12**, 43 (2020).
- [23] F. Mazzoncini, V. Cavina, G. M. Andolina, P. A. Erdman, and V. Giovannetti, Optimal control methods for quantum batteries, *Phys. Rev. A* **107**, 032218 (2023).
- [24] N. Behzadi and H. Kassani, Mechanism of controlling robust and stable charging of open quantum batteries, *J. Phys. A: Math. Theor.* **55**, 425303 (2022).
- [25] F. H. Kamin, F. T. Tabesh, S. Salimi, F. Kheirandish, and A. C. Santos, Non-Markovian effects on charging and self-discharging processes of quantum batteries, *New J. Phys.* **22**, 083007 (2020).
- [26] F. T. Tabesh, F. H. Kamin, and S. Salimi, Environment-mediated charging process of quantum batteries, *Phys. Rev. A* **102**, 052223 (2020).
- [27] A. C. Santos, B. Çakmak, S. Campbell, and N. T. Zinner, Stable adiabatic quantum batteries, *Phys. Rev. E* **100**, 032107 (2019).
- [28] F. Barra, Dissipative charging of a quantum battery, *Phys. Rev. Lett.* **122**, 210601 (2019).
- [29] M. Carrega, A. Crescente, D. Ferraro, and M. Sassetti, Dissipative dynamics of an open quantum battery, *New J. Phys.* **22**, 083085 (2020).
- [30] A. C. Santos, Quantum advantage of two-level batteries in self-discharging process, *Phys. Rev. E* **103**, 042118 (2021).
- [31] F. Zhao, F.-Q. Dou, and Q. Zhao, Quantum battery of interacting spins with environmental noise, *Phys. Rev. A* **103**, 033715 (2021).
- [32] C. D. Bruzewicz, J. Chiaverini, R. McConnell, and J. M. Sage, Trapped-ion quantum computing: progress and challenges, *Appl. Phys. Rev.* **6**, 021314 (2019).
- [33] P. Dřláz, J. J. García-Ripoll, B. Peropadre, J.-L. Orgiazzi, M. A. Yurtalan, R. Belyansky, C. M. Wilson, and A. Lupascu, Ultra-strong coupling of a single artificial atom to an electromagnetic continuum in the nonperturbative regime, *Nat. Phys.* **13**, 39 (2017).
- [34] K. Baumann, C. Guerlin, F. Brennecke, and T. Esslinger, The Dicke quantum phase transition with a superfluid gas in an optical cavity, *Nature (London)* **464**, 1301 (2010).
- [35] M. H. Devoret and R. J. Schoelkopf, Superconducting circuits for quantum information: An outlook, *Science* **339**, 1169 (2013).
- [36] W. Chang, T. R. Yang, H. Dong, L. Fu, X. Wang, and Y.-Y. Zhang, Optimal building block of multipartite quantum battery in the driven-dissipative charging, *New J. Phys.* **23**, 103026 (2021).
- [37] Y. Jiang, T. Chen, C. Xiao, K. Pan, G. Jin, Y. Yu, and A. Chen, Quantum battery based on hybrid field charging, *Entropy* **24**, 1821 (2022).
- [38] W. Zhang, S. Wang, C. Wu, and G. Wang, Quantum battery based on dipole-dipole interaction and external driving field, *Phys. Rev. E* **107**, 054125 (2023).
- [39] A. Crescente, M. Carrega, M. Sassetti, and D. Ferraro, Charging and energy fluctuations of a driven quantum battery, *New J. Phys.* **22**, 063057 (2020).
- [40] F. C. Binder, S. Vinjanampathy, K. Modi, and J. Goold, Quanta-cell: Powerful charging of quantum batteries, *New J. Phys.* **17**, 075015 (2015).
- [41] A. Solfanelli, L. Buffoni, A. Cuccoli, and M. Campisi, Maximal energy extraction via quantum measurement, *J. Stat. Mech.: Theory Exp.* (2019) 094003.
- [42] B. Mojaveri, A. Dehghani, and Z. Ahmadi, Maximal steady-state entanglement and perfect thermal rectification in non-equilibrium interacting XXZ chains, *Eur. Phys. J. Plus* **136**, 83 (2021).
- [43] X. Xu, K. Choo, V. Balachandran, and D. Poletti, Transport and energetic properties of a ring of interacting spins coupled to heat baths, *Entropy* **21**, 228 (2019).
- [44] F. Tacchino, T. F. F. Santos, D. Gerace, M. Campisi, and M. F. Santos, Charging a quantum battery via nonequilibrium heat current, *Phys. Rev. E* **102**, 062133 (2020).
- [45] R. Orbach, Linear antiferromagnetic chain with anisotropic coupling, *Phys. Rev.* **112**, 309 (1958).
- [46] X. Wang, Effects of anisotropy on thermal entanglement, *Phys. Lett. A* **281**, 101 (2001).
- [47] R. J. Baxter, *Exactly Solved Models in Statistical Mechanics* (Elsevier, Amsterdam, 2016).
- [48] V. E. Korepin, A. G. Izergin, and N. M. Bogoliubov, *Quantum Inverse Scattering Method and Correlation Functions* (Cambridge University Press, Cambridge, 1993).
- [49] H. P. Breuer and F. Petruccione, *The Theory of Open Quantum Systems* (Oxford University Press, Oxford, 2002).
- [50] A. Lenard, Thermodynamical proof of the Gibbs formula for elementary quantum systems, *J. Stat. Phys.* **19**, 575 (1978).
- [51] M. Perarnau-Llobet, K. V. Hovhannisyanyan, M. Huber, P. Skrzypczyk, N. Brunner, and A. Acín, Extractable work from correlations, *Phys. Rev. X* **5**, 041011 (2015).
- [52] M. Perarnau-Llobet, K. V. Hovhannisyanyan, M. Huber, P. Skrzypczyk, J. Tura, and A. Acín, Most energetic passive states, *Phys. Rev. E* **92**, 042147 (2015).
- [53] K. V. Hovhannisyanyan, M. Perarnau-Llobet, M. Huber, and A. Acn, Entanglement generation is not necessary for optimal work extraction, *Phys. Rev. Lett.* **111**, 240401 (2013).
- [54] W. Pusz and S. L. Woronowicz, Passive states and KMS states for general quantum systems, *Commun. Math. Phys.* **58**, 273 (1978).

- [55] F. H. Kamin, S. Salimi, and A. C. Santos, Exergy of passive states: Waste energy after ergotropy extraction, *Phys. Rev. E* **104**, 034134 (2021).
- [56] R. Kubo, Statistical-mechanical theory of irreversible processes. I. General theory and simple applications to magnetic and conduction problems, *J. Phys. Soc. Jpn.* **12**, 570 (1957).
- [57] P. C. Martin and J. Schwinger, Theory of many-particle systems. I, *Phys. Rev.* **115**, 1342 (1959).
- [58] R. Haag, N. M. Hugenholtz, and M. Winnink, On the equilibrium states in quantum statistical mechanics, *Commun. Math. Phys.* **5**, 215 (1967).
- [59] P. Skrzypczyk, R. Silva, and N. Brunner, Passivity, complete passivity, and virtual temperatures, *Phys. Rev. E* **91**, 052133 (2015).
- [60] V. Vedral, The role of relative entropy in quantum information theory, *Rev. Mod. Phys.* **74**, 197 (2002).
- [61] F. G. S. L. Brandão, M. Horodecki, J. Oppenheim, J. M. Renes, and R. W. Spekkens, Resource theory of quantum states out of thermal equilibrium, *Phys. Rev. Lett.* **111**, 250404 (2013).
- [62] M. Horodecki and J. Oppenheim, Fundamental limitations for quantum and nanoscale thermodynamics, *Nat. Commun.* **4**, 2059 (2013).